



HAL
open science

Sensitivity of the mixing-current technique in the detection of nano-mechanical displacement

Yue Wang

► **To cite this version:**

Yue Wang. Sensitivity of the mixing-current technique in the detection of nano-mechanical displacement. Other [cond-mat.other]. Université de Bordeaux, 2017. English. NNT : 2017BORD0659 . tel-01766467

HAL Id: tel-01766467

<https://theses.hal.science/tel-01766467>

Submitted on 13 Apr 2018

HAL is a multi-disciplinary open access archive for the deposit and dissemination of scientific research documents, whether they are published or not. The documents may come from teaching and research institutions in France or abroad, or from public or private research centers.

L'archive ouverte pluridisciplinaire **HAL**, est destinée au dépôt et à la diffusion de documents scientifiques de niveau recherche, publiés ou non, émanant des établissements d'enseignement et de recherche français ou étrangers, des laboratoires publics ou privés.

THÈSE PRÉSENTÉE
POUR OBTENIR LE GRADE DE
DOCTEUR DE
L'UNIVERSITÉ DE BORDEAUX

ÉCOLE DOCTORALE DES SCIENCES PHYSIQUES ET DE L'INGENIEUR
SPÉCIALITÉ : LASERS, MATIERE ET NANOSCIENCES

Par M. Wang YUE

**Sensitivité de la méthode dite de mélange des courants
pour la détection du déplacement nano-mécanique**

Sous la direction de : M. Fabio PISTOLESI

Soutenue le 8 Septembre 2017

Membres du jury :

M. COLLIN Eddy,	Chargé de Recherche, CNRS Grenoble	Rapporteur
M. HOUZET, Manuel,	Chercheur, CEA Grenoble	Rapporteur
M. KISELEV, Mikhael,	Professeur, ICTP, Trieste, Italie	Examineur
M. PISTOLESI, Fabio,	Directeur de Recherche, CNRS Talence	Directeur de thèse
M. WURGER Alois,	Professeur, Université de Bordeaux,	Examineur

Titre : Sensitivité de la méthode dite de mélange des courants pour la détection du déplacement nano-mécanique

Résumé : La détection des déplacements nano-mécaniques par les techniques de transport électronique a atteint un haut niveau de sensibilité et de polyvalence. Afin de détecter l'amplitude d'oscillation d'un oscillateur nano-mécanique, une technique largement utilisée consiste à coupler ce mouvement de façon capacitive à un transistor à un seul électron ou, plus généralement, à un dispositif de transport, et à détecter la modulation haute fréquence du courant à travers le mélange non linéaire avec un signal électrique à une fréquence légèrement désaccordée. Cette méthode, connue sous le nom de technique de mélange des courants, est utilisée notamment pour la détection de nanotubes de carbone suspendus et s'est avérée particulièrement efficace, ce qui a permis d'obtenir des records de sensibilité dans la détection de masse et de force. Dans cette thèse nous étudions théoriquement les conditions qui limitent la sensibilité de cette méthode dans différents types de dispositifs de transport. La sensibilité est un compromis entre le bruit, le bruit de rétroaction et la fonction de réponse. Cette dernière est proportionnel au couplage électromécanique. Pour ces raisons dans la thèse, nous étudions la fonction de réponse, l'effet des fluctuations de courant et de déplacement (back-action) dans les dispositifs de détection suivants: (i) le transistor métallique à électron unique, (ii) le transistor à un seul niveau électronique et (iii) le point quantique cohérent. La sensibilité optimale est obtenue, comme d'habitude, lorsque la rétroaction du dispositif de détection est égale au bruit du signal intrinsèque, ce qui, dans notre cas, est le bruit en courant. Nous avons constaté que les valeurs optimales typiques du couplage sont obtenues dans la limite de couplage fort, où une forte renormalisation de la fréquence de résonance est observée et une bistabilité de l'oscillateur mécanique est présente [comme discuté dans G. Micchi, R. Avriller, F. Pistolesi, Phys. Rev. Lett. 115, 206802 (2015)]. Nous trouvons donc des limites supérieures à la sensibilité de la technique de détection de mélange des courants. Nous considérons également comment la technique du mélange des courants est modifiée dans la limite où le taux de transmission tunnel devient comparable à la fréquence de résonance de l'oscillateur mécanique.

Mots clés : Systèmes nano-électromécaniques, transport quantique, bruit actuel, détection, nanotubes de carbone, fluctuations

Title : Sensitivity of the mixing-current technique in the detection of nano-mechanical displacement

Abstract :

Detection of nanomechanical displacement by electronic transport techniques has reached a high level of sensitivity and versatility. In order to detect the amplitude of oscillation of a nanomechanical oscillator, a widely used technique consists of coupling this motion capacitively to a single-electron transistor or, more generally, to a transport device, and to detect the high-frequency modulation of the current through the nonlinear mixing with an electric signal at a slightly detuned frequency. This method, known as mixing-current technique, is employed in particular for the detection of suspended carbon nanotubes and has proven to be particularly successful leading to record sensitivities of mass and force detection. In this thesis we study theoretically the limiting conditions on the sensitivity of this method in different kind of transport devices. The sensitivity is a compromise between the noise, the back-action noise, and the response function. The latter is proportional to the electromechanical coupling. For these reasons in the thesis we study the response function, the effect of current and displacement (back-action) fluctuations for the following detection devices: (i) the metallic single electron transistor, (ii) the single-electronic level single electron transistor, and (iii) the coherent transport quantum dot. The optimal sensitivity is obtained, as usual, when the back-action of the detection device equals the intrinsic signal noise that, in our case, is the current noise. We found that the typical optimal values of the coupling are obtained in the strong coupling limit, where a strong renormalization of the resonating frequency is observed and a bistability of the mechanical oscillator is present [as discussed in G. Micchi, R. Avriller, F. Pistolesi, Phys. Rev. Lett. 115, 206802 (2015)]. We thus find upper bounds to the sensitivity of the mixing-current detection technique. We also consider how the mixing-current technique is modified in the limit where the tunneling rate becomes comparable to the resonating frequency of the mechanical oscillator.

Keywords : nano-electromechanical systems, quantum transport, current noise, sensing, carbon nanotubes, fluctuations

Unité de recherche

Laboratoire d'Ondes et Matière d'Aquitaine (LOMA), Université de Bordeaux and CNRS, 351 cours de la libération, building A4N, 33405, Talence, CEDEX, FRANCE

Acknowledgements

I begin to realize that the life in France will be over when I start to write this thesis, the pictures of the past life scenes come up in my brain. Arrive at this step, that is not easy for me, a Chinese, who has never been in a foreign country before. This work goes smoothly without the help of many people, who are very kind, friendly and helpful.

Firstly, I would like to give my best sincerely thanks to my supervisor, Mr. Fabio Postolesi. His profound academic attainments and strong sense of responsibility give me very deeply impression, inspiring me how to be a good scientist. His patience and support are around every discussion, providing me with ideas and solutions to the problems during these few years. Furthermore, he pays his attention on my life in France and encourages me to make more friends, more communicate with others. In a word, I am very luck for finishing my Phd project under the supervision of Professor Fabio Pistolessi.

Then I would like to thank the all the other Phd students, postdocs, and friends in Bordeaux. Especially my colleague Gianluca Micchi, without his help in the numerical calculation, my second project could not be finished in time. My appreciation goes to all the LOMA members, both past and present, for giving me a wonderful memory.

Finally, my deepest gratitude goes to my family, my mum and brother, their support and encouragement always give me a powerful driving force throughout my time in Bordeaux.

Contents

Acknowledgements	v
Contents	vi
1 Introduction	1
2 Electrostatics in a Single Electron Transistor	5
3 Mixing technique and response function	11
4 Added Noise to the Signal	15
4.1 Shot-noise and thermal current fluctuations	16
4.2 Displacement back-action fluctuations	17
5 Fast oscillator	21
6 Incoherent tunnelling regime	29
6.1 The metallic dot single-electron transistor	29
6.1.1 Low temperature case	29
6.1.2 Finite temperature case	36
6.2 The single-electronic level SET	39
7 Coherent tunnelling regime	43
7.1 Model	44
7.2 Current noise sources	47
7.2.1 Intrinsic electronic current noise	47
7.2.2 Back-action current noise	48
7.3 Weak coupling regime	48
7.4 Non-linear regime	51
7.4.1 Weakly non-linear regime	53
7.5 Numerical evaluation of the fluctuations	58
8 Conclusions	63

A Full Counting Statistics for periodically modulated system	67
A.1 Model and the rate equation	67
A.2 Solution of the equation	70
References	75

Chapter 1

Introduction

Macroscopic electromechanical systems are ubiquitous in our daily life. A minimal definition of an electromechanical system is a mechanical system that is actuated or detected by an electronic system. In this category we thus have electric motors, loudspeakers, microphones, high-power relays, etc. At the macroscopic scale we are used to exploit electro-mechanical devices. In many cases the miniaturization of such systems is simply not possible, since the task performed is on a macroscopic scale (like for high power devices). The current technology allows to fabricate the electro-mechanical devices on the nanometer scale and the reduction of the size of the device can be very useful. This is the case, for instance, for the detectors, for which a drastic reduction of the size can lead to a reduction of the dissipation, the increase of the sensitivity, and finally to completely new functionalities. Nano Electro Mechanical Systems (NEMS) hold thus promise for a number of technological applications. Their small size of the devices is at the origin of their sensibility and to their capability of local detection, for instance a tiny force is sufficient to put into motion a nanometer scale oscillator.

Nano-electromechanical systems have thus great potentials as ultra-sensitive detectors for several physical quantities. Recent advances allowed to reach record sensitivity in mass sensing [1-3]. This has been possible by the detection of the frequency shift of ultralight oscillators when an additional mass is attached to it. Other examples concern the detection of the tiny magnetic field generated by nuclear spins. This can be done by the opto-mechanical detection of the force generated by the magnetic dipoles [4], but

also with electro-mechanical means [5], or by coupling to two-level systems [6–8]. The force sensitivity of the device is then the limiting factor for the sensitivity, and again recent advances showed that it is possible to obtain record force sensing with carbon-nanotube oscillators [9, 10]. At the same time nano-mechanical oscillators can be so small that interaction between electronic and mechanical degrees of freedom may lead to new and unexpected phenomena [11–15], like the blockade of the current [16–19], cooling [20–22], heating [23], phonon lasing [24], noise squeezing [25], or unusual mechanical response [26, 27].

In order to exploit nanomechanical resonators, or to study their properties, detection of mechanical motion is crucial. Most detection methods exploiting electronic transport are based on the high sensitivity of single-electron transistors (SET) to a variation of the gate charge. By coupling capacitively the oscillator to the gate of the SET it is possible to detect the motion of the oscillator with a high accuracy [28]. The method has been used also to cool the oscillator by the back-action of the electronic transport [29]. The main difficulty of the method stems from the high frequency character of the oscillator motion that is typically in the 100 MHz-1 GHz range. Due to the high impedance of the SET, it is more convenient to down-convert the signal to lower frequency before extracting it. This can be achieved by non-linear mixing the mechanically generated modulation with a second high-frequency signal injected between source and drain. The signal at the difference of the two frequencies can be extracted and measured. To our knowledge, for nanomechanical resonators this method was implemented in metallic SET by the group of A. Cleland back in 2003 [30]. It was later adapted to the detection of carbon nanotube by the group of P.L. McEuen [31]. It then became the method of choice for carbon nanotubes, leading to several breakthroughs: the observation of the first single-electron backaction effects in carbon nanotubes [32, 33], ultrasensitive mass detection [2, 3], the detection of the charge response function in quantum dot [34], the detection of magnetic molecules [35, 36], and the observation of decoherence of mechanical motion [37]. The same method can also be implemented by frequency modulation [38]. It is clear that the technique is powerful and that it will continue to be used both for fundamental research and for applications. The question we want to address in this Thesis is which is the ultimate resolution that can be reached with this kind of detection. In order to

do this we investigated three main issues. The first one is how to optimize the response function, that is the quantity $\partial I_{\text{mx}}/\partial x_m$, where I_{mx} is the measured signal, the mixing current, and x_m the amplitude of the mechanical oscillation. The second one is to study the effect of current and mechanical fluctuations. These contribute to the fluctuation of the measured signal and in the end are at the origin of the signal to noise ratio. The third is to consider the case of a mechanical oscillator with a resonating frequency ω_m faster than the typical tunneling rate of the electrons Γ .

The Thesis is organized as follows. In Chapter 2 we recall few results concerning the electrostatics of a SET. In Chapter 3 we describe the mixing technique and define the main quantities that will be calculated in the remainder of the Thesis. In Chapter 3 we describe the mixing technique and define the response function. In Chapter 4 we describe the limitations induced by the current fluctuations. We define the main quantities that will be calculated in the remainder of the Thesis. In Chapter 5 we derive the transport equations for the case of a fast oscillator, i.e. the case when the resonating frequency ω_0 of the oscillator is much larger than the electronic tunnelling rate Γ . In Chapter 6 we apply the previous definitions and investigate the sensitivity of a detection device in the incoherent tunnelling regime of $\Gamma \ll k_B T$, where T is the temperature at which the electronic system is operated. In Chapter 7 we investigate the case of a coherent transport device (valid for $k_B T \ll \Gamma$). This chapter considers in details the presence of a bistability for strong coupling that has been investigate recently [26]. Finally in Chapter 8 we present our conclusions.

Chapter 2

Electrostatics in a Single Electron Transistor

The single-electron tunneling and Coulomb Blockade are both important physical phenomena in the NEMS research field. Firstly, let us give a short introduction to the single-electron tunneling. This phenomenon can be observed in tunnel junctions when the lateral size of the junction is so small that the Coulomb energy E_C associated to the charging of the capacitance by a single electron becomes of the order of the temperature T at which the experiment is performed. The quantity E_C is given for a single junction by simply $e^2/2C$, where e is the electron charge and C is the capacitance of the junction. In the case of a double junction, the electron in the central island can also block the tunneling of a second one. That means one electron tunnels one at a time in such a junction. We call this sequential tunneling.

We present now a brief derivation of the electrostatic energy variation for the tunneling of an electron in a single electron transistor [39]. The electric scheme is presented in Fig. 2.1 where the potentials of the left, right, and gate leads are defined as V_L , V_R , and V_g , respectively. In the same way the charge on each capacitance (on the leads side) is indicated with Q_i with $i = L, R$, and g . Defining V_I the potential of the island one has

$$Q_i = (V_i - V_I)C_i. \quad (2.1)$$

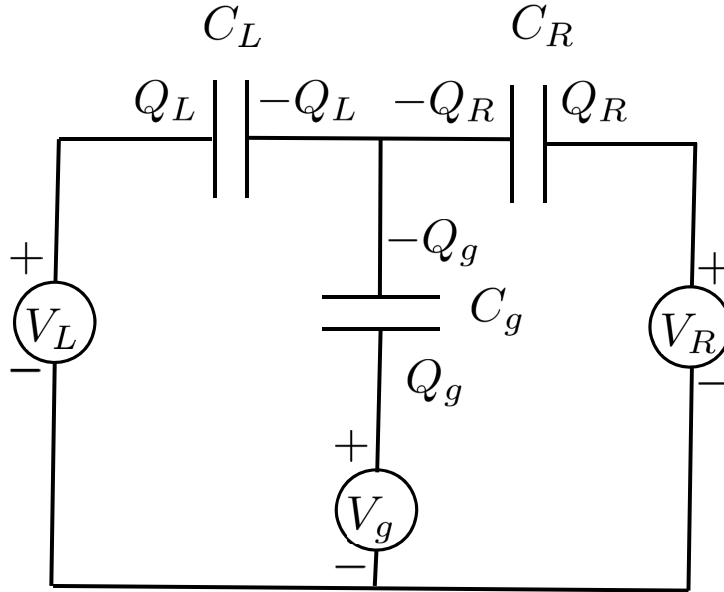


FIGURE 2.1: Electric scheme of a single electron transistor

Summing the three equations one obtains immediately the expression for the potential on the island:

$$V_I = \left(\sum_i C_i V_i + Q \right) / C_\Sigma, \quad (2.2)$$

where $C_\Sigma = \sum_i C_i$ and $Q = -\sum_i Q_i$ is the total charge on the island. The total electrostatic energy

$$E_e(Q) = \sum_i \frac{Q_i^2}{2C_i} = \frac{Q^2}{2C_\Sigma} + \text{constant}, \quad (2.3)$$

where the constant term is $\sum_i C_i V_i^2 / 2 - (\sum_i C_i V_i)^2 / 2C_\Sigma$. From Eq. (2.1) and Eq. (2.2) one then finds that adding a charge q on the island will change the charge on each capacitor plate of

$$\delta Q_i = -\frac{q C_i}{C_\Sigma}. \quad (2.4)$$

The total electrostatic energy variation (final energy minus initial energy) for the transfer of an electron from the left electrode on the island is then given by the variation of the total electrostatic energy plus the the work done by the voltage sources. These can be more easily evaluated by treating the sources as large capacitors. The variation of the charge of each capacitor has to satisfy:

$$\delta Q_l + \delta Q_L = -q, \quad (2.5)$$

$$\delta Q = 0, \quad (2.6)$$

$$\delta Q_r + \delta Q_R = 0, \quad (2.7)$$

$$\delta Q_g + \delta Q_G = 0. \quad (2.8)$$

Here we indicate $Q_{l,r,g}$ the charge on the each source where the capacitance in the limit $C_{l,r,g} \rightarrow \infty$.

This finally gives for the work of the sources: $-\sum_i V_i \delta Q_i$, with

$$\delta Q_i = eC_i/C_\Sigma \text{ for } i \neq L \text{ and } \delta Q_L = eC_L/C_\Sigma - e. \quad (2.9)$$

We thus find for the total energy variation:

$$\Delta E_L^\pm = E_e(Q - e) - E_e(Q) - e \sum_i V_i \frac{C_i}{C_\Sigma} + eV_L. \quad (2.10)$$

The general expression reads then:

$$\Delta E_{L,R}^\pm = -e \frac{(-e \pm 2Q)}{2C_\Sigma} \mp \frac{e}{C_\Sigma} \left(\sum_i V_i C_i - C_\Sigma V_{L,R} \right). \quad (2.11)$$

The variation of the energy depends only on the difference of the three potentials, we can thus choose to express it in terms of :

$$V = V_R - V_L, \quad (2.12)$$

$$V'_g = V_g - (V_L + V_R)/2. \quad (2.13)$$

For simplicity we write the expressions in the symmetric case of $C_L = C_R = C$:

$$\Delta E_L^\pm = \frac{e}{2C_\Sigma} (e \mp 2Q) \mp \frac{e}{C_\Sigma} (C'V + C_g V'_g), \quad (2.14)$$

$$\Delta E_R^\pm = \frac{e}{2C_\Sigma} (e \mp 2Q) \mp \frac{e}{C_\Sigma} (-C'V + C_g V'_g) \quad (2.15)$$

with $C' = C + C_g/2$. Typically V is very small, while V'_g can be very large, in particular $V'_g C_g/e = n_g$ is normally regarded as finite, while $C_g \rightarrow 0$ and $V'_g \rightarrow \infty$. In the following

of the Thesis we will consider position dependent gate capacitance ($C_g(x)$). For the same reasons we can normally neglect the displacement dependence induced by $C_g(x)$ in C' or C_Σ , while it is necessary to keep the x dependence in $C_g(x)$ that appears in the expression $C_g V'_g$.

Let now focus on the four energy variations associated with the change of the number of electrons in the dot between the two states N and $N + 1$. We need $\Delta E_{L,R}^+(N) = -\Delta E_{L,R}^-(N + 1)$ that can be explicitly written as:

$$\Delta E^+(N)_{L,R} = -\frac{e^2}{C_\Sigma}(n_g \pm v - N - 1/2), \quad (2.16)$$

with $n_g = C_g V'_g/e$ and $v = C'V/e$. The expression of the tunneling rate is obtained then by the Fermi golden rule:

$$\Gamma^{\alpha\pm} = \frac{k_B T}{e^2 R_\alpha} h(\Delta_\alpha^\pm/k_B T), \quad (2.17)$$

with $h(x) = -x/(1 - e^x)$. In particular for $T \rightarrow 0$ the expression for the rate becomes simply

$$\Gamma^{\alpha\pm} = -\Delta_\alpha^\pm/e^2 R_\alpha \theta(-\Delta_\alpha^\pm), \quad (2.18)$$

These expressions allow to obtain the tunneling rates necessary for the calculations presented in the reminder of the Thesis.

We can now find the region in the space $n_g - v$ where the current is blocked with the island in the state with N electrons. This is defined by the values of n_g and v for which $\Delta E^+(N)_{L,R} > 0$ and $\Delta E^-(N)_{L,R} > 0$, *i.e.* it costs energy to add or to remove one electron from the island. Explicitly it reads:

$$\Delta E_L^+(N) > 0 \quad \text{for} \quad v < -n_g + N + 1/2, \quad (2.19)$$

$$\Delta E_L^-(N) > 0 \quad \text{for} \quad v > -n_g + N - 1/2, \quad (2.20)$$

$$\Delta E_R^+(N) > 0 \quad \text{for} \quad v > n_g - N - 1/2, \quad (2.21)$$

$$\Delta E_R^-(N) > 0 \quad \text{for} \quad v < n_g - N + 1/2. \quad (2.22)$$

Fig. 2.2 shows the region of current blockade. The same shape is repeated periodically by increasing n_b by one unit each time.

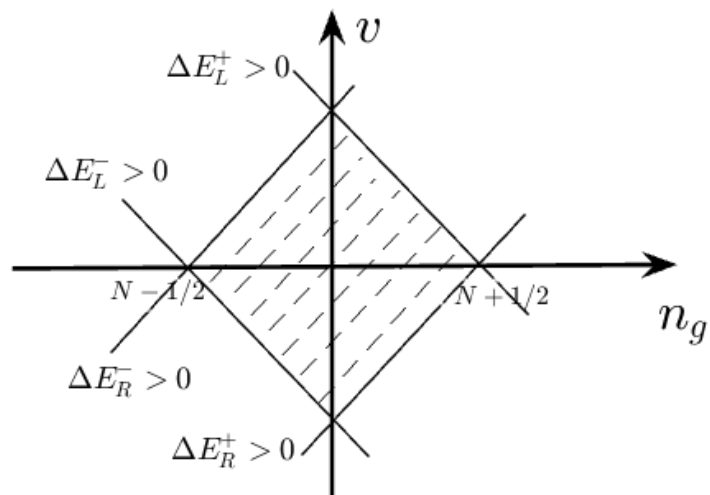


FIGURE 2.2: The region of stability with respect to all possible tunnelling process (the variation of the energy is always positive)

Chapter 3

Mixing technique and response function

Let us begin by describing the typical system used to measure the oscillation amplitude of a mechanical oscillator by detection of the mixing current [30–33]. As shown in Fig. 3.1 a conducting oscillator is capacitively coupled to the central island of a single-electron transistor: its displacement modulates thus the the gate capacitance $C_g(x)$, where $x(t)$ is the displacement of the oscillator. We assume the presence of a single mechanical mode whose displacement is parametrized by x , a generalized coordinate with the dimensions of a length. We will consider that the SET is operated in the incoherent transport regime valid for $\hbar\Gamma \ll k_B T$, where Γ is the electron tunnelling rate and T the temperature (\hbar and k_B are the reduced Planck constant and the Boltzmann constant, respectively). This is the standard case for nano-mechanical devices. The current I through the device can be obtained by using the Master equation and in general it can be expressed as a function of the source-drain bias voltage V and on the gate charge $n_g = C_g(x)V_g/e$, where V_g is the gate voltage (see Chapter 2 for a short derivation). The current reads thus:

$$I = I(V, n_g). \quad (3.1)$$

In this section we want to obtain the current response of the system when both V and V_g are modulated at two slightly different frequencies ω_1 and ω_2 , both much smaller than

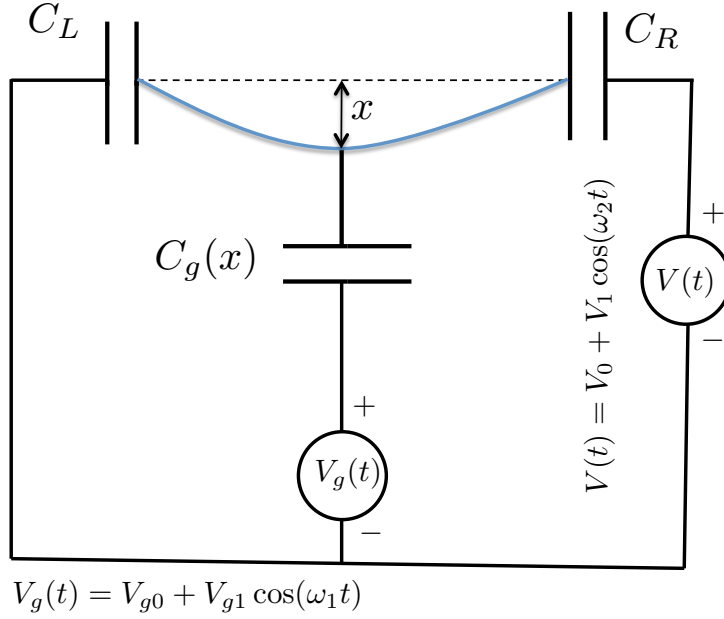


FIGURE 3.1: Schematic of the typical experimental set-up used to measure the displacement of a mechanical oscillator by detection of the mixing current (adapted from Ref. [31])

Γ . We write

$$V_g(t) = V_{g0} + V_{g1}(t), \quad V(t) = V_0 + V_1(t), \quad (3.2)$$

where

$$V_{g1}(t) = V_{g1} \cos(\omega_1 t), \quad V_1(t) = V_1 \cos(\omega_2 t), \quad (3.3)$$

Choosing ω_1 close to the mechanical resonating frequency ω_m allows to drive the resonator, while ω_2 is chosen close to ω_1 with $|\omega_1 - \omega_2| \ll \omega_{1,2}$. In general the requirement is that $|\omega_1 - \omega_2|$ is much smaller than the bandwidth of the electronic circuit that is typically dominated by the RC -time of the single electron transistor. The variation of the gate voltage modulates the charge on the suspended part and thus induces an oscillating force [see also Eq. (7.33) in the following]. For small driving amplitude the oscillator responds linearly to the external drive:

$$x(t) = x_m \cos(\omega_1 t + \phi), \quad (3.4)$$

where we always measure x from its equilibrium position. (Note that in general x_m and ϕ depend on the driving frequency ω_1 .) The modulation of V_g induces thus the following

modulation of n_g at linear order in the driving:

$$n_g(t) = n_{g0} + \frac{C_g V_{g1}}{e} \cos(\omega_1 t) + \frac{C'_g x_m V_{g0}}{e} \cos(\omega_1 t + \phi), \quad (3.5)$$

where $C'_g \equiv dC_g/dx$. It is convenient to introduce a length scale by defining $L = C_g/C'_g$. From geometric considerations L has to be of the order of the distance of the gate from the oscillator, thus typically undreds of nm. The fluctuating part of n_g can then be written as

$$n_{g1}(t) = n_{g0} \left[\frac{V_{g1}}{V_{g0}} \cos(\omega_1 t) + \frac{x_m}{L} \cos(\omega_1 t + \phi) \right], \quad (3.6)$$

where $n_{g0} = C_g V_{g0}/e$. The mechanical term (x_m/L) has a strong frequency dependence close to the mechanical resonance, and can thus be distinguished by the back-ground electrostatic term (V_{g1}/V_{g0}). The two contributions to the modulation of the gate charge can be combined in a single cosine term:

$$n_{g1}(t) = n_{g1} \cos(\omega_1 t + \varphi). \quad (3.7)$$

Assuming now that the oscillator frequency ω_m , and thus also ω_1 and ω_2 , are much smaller than the typical tunneling rate Γ , one can use Eq. (3.1) to obtain the time dependent current in presence of time-dependent V and n_g . For small modulation amplitude we Taylor expand Eq. (3.1) to second order in V_1 and n_{g1} obtaining

$$\begin{aligned} I(t) = & I(V_0, V_{g0}) + \frac{\partial I}{\partial V} V_1(t) + \frac{\partial I}{\partial n_g} n_{g1}(t) \\ & + \frac{1}{2} \frac{\partial^2 I}{\partial V^2} V_1^2(t) + \frac{\partial^2 I}{\partial V \partial n_g} V_1(t) n_{g1}(t) + \frac{1}{2} \frac{\partial^2 I}{\partial n_g^2} n_{g1}^2(t) + \dots \end{aligned} \quad (3.8)$$

Only the term proportional to $\partial^2 I / \partial V \partial n_g$ has a component that oscillates at the frequency $\omega_\Delta = \omega_1 - \omega_2$. This signal can be extracted by a standard lock-in technique that essentially allows to measure the quantity I_{mx} :

$$I_{\text{mx}}^c = \int_0^{T_m} \frac{dt}{T_m} I(t) \cos[\omega_\Delta t]. \quad (3.9)$$

The other quadrature I_{mx}^s with $\sin(\omega_\Delta t)$ is defined in a similar way. Averaging over a long measurement time $T_m \gg 1/\omega_\Delta$ one obtains:

$$I_{\text{mx}}^c = \frac{V_1}{4} \frac{\partial^2 I}{\partial V \partial n_g} [C_g V_{g1} + C'_g V_{g0} x_m \cos \phi] , \quad (3.10)$$

$$I_{\text{mx}}^s = -\frac{V_1}{4} \frac{\partial^2 I}{\partial V \partial n_g} C'_g V_{g0} x_m \sin \phi . \quad (3.11)$$

The detector gain with respect to the two quadrature of x_m is thus:

$$\lambda = \frac{1}{4e} \frac{\partial^2 I}{\partial V \partial n_g} C'_g V_{g0} V_1 . \quad (3.12)$$

It measures the sensitivity of the mixing current signal with respect to the two quadratures of x . This quantity depends on the particular bias conditions of the SET, and will be studied in some details in Section 6.1 and 6.2 for two explicit models. Note also that in order to obtain λ we need only the static expression for the current. This assumes that the electronic mechanism is much faster than the time dependence of the driving. In order to describe the case of a fast oscillator (to be discussed in Chapter 5 we will need a detailed description of the charge dynamics, and the response function will be no more expressed only in terms of derivatives of the static non-linear current voltage characteristics.

Chapter 4

Added Noise to the Signal

Expression (3.12) assumes a deterministic evolution of both the current and the displacement of the oscillator $x(t)$. In practice both quantity fluctuate, the first due to shot or thermal noise, and the second due to stochastic fluctuations induced either by the bias voltage or by the thermal fluctuations. The fluctuations induced by the measurement voltage are normally indicated as back-action fluctuations, since they are due to the measurement process. In general one can then write the value of I_{mx} in a specific time region as follows:

$$(I_{\text{mx}}^c)_n = \int_{nT_m}^{(n+1)T_m} [I(t) + \delta I(t)] \cos(\omega_{\Delta} t) dt, \quad (4.1)$$

(we write the expression for I_{mx}^c , the one for I_{mx}^s is similar) where $\delta I(t)$ and $I(t)$ are the stochastic and deterministic (in phase with the external drive) part, respectively. We can define the time dependent mixing current as $I_{\text{mx}}^c(t) = (I_{\text{mx}}^c)_{[t/T_m]}$, where $[\alpha]$ stands here for the integer part of α . In terms of that the spectral density of the fluctuation of I_{mx}^c reads:

$$S_{\text{mx}}(\omega) = \int_{-\infty}^{+\infty} dt e^{i\omega t} [\langle I_{\text{mx}}^c(t) I_{\text{mx}}^c(0) \rangle - \langle I_{\text{mx}}^c \rangle^2]. \quad (4.2)$$

We assume that the measuring time is much longer than any correlation time of the quantity $\delta I(t)$. Different sections of the measurement time are thus uncorrelated and we

can write:

$$S_{\text{mx}}(\omega) = \int_0^{T_m} dt e^{i\omega t} \int_0^{T_m} \frac{dt_1}{T_m} \int_0^{T_m} \frac{dt_2}{T_m} \cos(\omega_\Delta t_1) \cos(\omega_\Delta t_2) \langle \delta I(t_1) \delta I(t_2) \rangle. \quad (4.3)$$

Defining

$$S_I(\omega = 0) = 2 \int_{-\infty}^{+\infty} dt \langle \delta I(t) \delta I(0) \rangle, \quad (4.4)$$

here the numerical factor 2 is conventional for the current-noise spectrum, then we have

$$S_{\text{mx}}(\omega) = \frac{1}{4} S_I(\omega = 0) \frac{(e^{i\omega T_m} - 1)}{i\omega T_m} \approx \frac{1}{4} S_I(\omega = 0). \quad (4.5)$$

Thus the mixing-current low-frequency noise is given simply by the low-frequency current noise spectrum S_{II} . The factor of 4 comes from a different definition of the correlation functions and from the fact that we are collecting a single quadrature. The current noise can have different sources, we consider in the following the two main ones.

4.1 Shot-noise and thermal current fluctuations

The current fluctuates due to the discrete nature of the the charge. This is characterized by the current-spectral function (for time-independent bias and gate voltages):

$$S_I^{\text{shot}}(\omega) = 2 \int dt e^{i\omega t} \langle \delta I(t) \delta I(0) \rangle, \quad (4.6)$$

where $\delta I(t) = I(t) - \langle I \rangle$. For the case of a SET the current spectral function is well known [40]. As shown there it has a frequency dependent part at low frequency on the scale of the typical tunneling rate Γ . This implies that the correlation function is short ranged with respect to the measuring time T_m . Actually it is typically even short ranged with respect to the time dependence of x and of the V or V_g potentials. Its value can thus be obtained adiabatically, by assuming these parameters to be static. We only need its low frequency part that can, in general, be expressed in terms of the Fano factor \mathcal{F}

and the current I :

$$S_I^{\text{shot}}(\omega = 0) = 2e\mathcal{F}I, \quad (4.7)$$

where \mathcal{F} depends on the details of the SET. In the tunnelling limit of uncorrelated tunneling $\mathcal{F} = 1$, in most other cases the Fano factor is typically of the order of 1.

4.2 Displacement back-action fluctuations

The electrons that cross the structure modify the charge on the gate that in turn modifies the force acting on the oscillator. This stochastic force, that has the same origin of the current-shot noise, induces fluctuations of the displacement, that changes in a much slower way, since the oscillator responds to an external force on the time scale given by its damping coefficient γ [13, 18, 41, 42]. In order to keep the assumption that different averages over the measuring times are uncorrelated one needs $T_m\gamma \gg 1$. In principle, for very high- Q resonators the approximation should be reconsidered.

Let's begin by considering the force acting on the oscillator as a consequence of a variation of the charge on the gate. A recall of the basic expressions for the electrostatic energy is given in the Chapter 2 and Fig 3.1 there shows the electrical scheme. The force acting on the oscillator is given by the derivative of the electrostatic energy performed at constant charge:

$$F = -Q_g^2 \frac{\partial}{\partial x} \frac{1}{2C_g(x)} = \frac{Q_g^2 C'_g}{2C_g^2}, \quad (4.8)$$

where Q_g is the charge on the gate voltage (Fig.3.1). The fluctuation of the force $\delta F(t)$ due to fluctuation of Q_g reads thus:

$$\delta F(t) = \frac{Q_g C'_g}{C_g^2} \delta Q_g(t). \quad (4.9)$$

In general the variation of the charge on the gate is proportional to the variation of the charge on the central island of the SET. By an elementary electrostatic calculation (see Chapter 2) $\delta Q_g/e = (C_g/C_\Sigma)\delta n$, where $C_\Sigma = C_g + C_L + C_R$ is the sum of the capacitances of the central island to all the electrodes and $-ne$ is the total charge on the island. In

conclusion one finds that

$$\delta F(t) = F_0 \delta n(t) \quad (4.10)$$

with

$$F_0 = \frac{Q_g e C'_g}{C_g C_\Sigma} = 2 \frac{Q_g}{e} \frac{E_C}{L} \quad (4.11)$$

the force acting on the oscillator when an electron is added to the dot and with $E_C = e^2/(2C_\Sigma)$ the Coulomb energy of the SET. Note that F_0 is a crucial parameter, since it constitutes the electro-mechanical coupling constant [18, 26]. One can estimate the typical value of F_0 : $Q_g/e = 10-100$, $E_C = 1$ K, $L = 100$ nm, thus $F_0 \approx 10^{-11}-10^{-12}$ N.

The correlation function of the stochastic force acting on the resonator [$S_F(t) = \langle \delta F(t) \delta F(0) \rangle$] is thus simply proportional to the correlation function of the charge on the island [$S_{\delta n}(t) = \langle \delta n(t) \delta n(0) \rangle$]:

$$S_F(t) = F_0^2 S_n(t), \quad (4.12)$$

that can be calculated by the standard method of the master equation. For the case of a metallic dot see for instance Refs. [18, 43]. Its Fourier transform has a Lorentzian form with a width on the scale of Γ . Thus this force act as a white noise on the slow oscillator.

Let's now turn to the displacement correlation function. In order to evaluate it we use a simple Langevin approach [11, 16]. We neglect the driving, since we are interested in the low frequency response. The Langevin equation reads

$$m\ddot{x} + m\gamma\dot{x} + kx = \delta F(t), \quad (4.13)$$

where m is the (effective mass) of the oscillator mode considered, γ the damping coefficient, and k the effective spring constant. The stochastic force generated by the electrons is also at the origin of the damping coefficient. In general other effects participate, but close to the degeneracy point of the SET, when the current is maximal, the electronic contribution to the damping can dominate, as observed experimentally in Ref. [35]. We will assume thus that γ is due only to the electronic damping. In equilibrium the fluctuation-dissipation theorem gives

$$S_{\delta F}(\omega = 0) = 2\gamma m k_B T. \quad (4.14)$$

For finite $eV \gg k_B T$, the system is out of equilibrium and one has to evaluate explicitly γ and $S_{\delta F}$ from a direct calculation of $S_F(\omega)$. As shown in Ref. [44] $2m\hbar\gamma = dS_F(\omega)/d\omega|_{\omega=0}$. One can then always define an effective temperature by the relation $S_F(\omega = 0) = 2\gamma m k_B T_{\text{eff}}$, since the oscillator has a very sharp response in frequency and the correlation functions are flat on that scale, one can always interpret the ratio of the fluctuation and the dissipation as an effective temperature. In the case of the SET it has been shown that the typical value of $k_B T_{\text{eff}}$ is of the order of eV , when $k_B T \ll eV$ [13].

The Langevin equation (4.13) can then be solved by Fourier transform giving

$$S_x(\omega) = \langle x(\omega)x(-\omega) \rangle = \frac{F_0^2 S_n(\omega)}{m^2 |\omega_m^2 - \omega^2 - i\gamma\omega|^2} \quad (4.15)$$

and in particular in the low-frequency limit:

$$S_x(\omega = 0) = \frac{F_0^2 S_n(\omega = 0)}{m^2 \omega_m^4}. \quad (4.16)$$

We can now use the expansion (3.8) to find the lowest order contribution of the stochastic fluctuations of $x(t)$ to the current. We denote these fluctuations $\delta x(t)$ to distinguish them from the time-dependent average induced by the external driving:

$$\delta I(t) = \frac{\partial I}{\partial n_g} \frac{V_{g0} C'_g}{e} \delta x(t) + \dots \quad (4.17)$$

The back-action current noise is then

$$S_I^{\text{ba}}(\omega) = 2 \left(\frac{\partial I}{\partial n_g} \frac{F_0 n_g}{kL} \right)^2 S_n(\omega = 0). \quad (4.18)$$

As discussed in Refs. [19, 45] the mechanical back-action noise can be very strong and induce effective giant Fano factors. In Appendix A, we afford another method to obtain the fluctuations of the mixing current technique through the full counting statistics of charge transport in SET driven by two harmonic signals. Finally the measurement added noise can be obtained as is done for the amplifiers [46], by dividing the fluctuation

of the current signal by the amplifier gain squared. This gives:

$$S_x^{\text{add}} = \frac{S_{\text{mx}}}{\lambda^2} = \frac{S_I^{\text{shot}} + S_I^{\text{ba}}}{4\lambda^2}. \quad (4.19)$$

This quantity gives the upper bound on the detection sensibility, since the limitations considered are intrinsic to the detection method. We will evaluate explicitly these quantities for two specific models in sections [6.1](#) and [6.2](#).

Chapter 5

Fast oscillator

In this chapter we relax the condition $\omega_m \ll \Gamma$ for the calculation of the mixing current. We assume $\hbar\Gamma, \hbar\omega_m \ll k_B T$, the electronic transport is then described by sequential transport and we will find the mixing current to lowest non-vanishing order in the amplitude of the oscillating field by making use of a master equation description.

Let's begin by introducing in some details the electron tunnelling description. We assume that the only available charge states on the island are those associated with two charge states Ne and $(N + 1)e$. We will call these two states 0 and 1. The state of the SET is thus fully described by the probabilities of one of these two states to be realized: P_n , with $n = 0, 1$. We define $\Gamma^{L+(-)}$ as the rate for adding (subtracting) one electron on (from) the central island through the left tunnel junction. Similarly we define $\Gamma^{R+(-)}$ for the right junction. We define also $\Gamma^\alpha = \Gamma^{L\alpha} + \Gamma^{R\alpha}$, with $\alpha = \pm$, $\Gamma^L = \Gamma^{L+} + \Gamma^{L-}$, $\Gamma^R = \Gamma^{R+} + \Gamma^{R-}$, and $\Gamma^T = \Gamma^+ + \Gamma^-$. The master equation for the probability reads ($\dot{P} \equiv dP/dt$):

$$\dot{P}_0 = -\Gamma^+ P_0 + \Gamma^- P_1, \quad (5.1)$$

$$\dot{P}_1 = \Gamma^+ P_0 - \Gamma^- P_1. \quad (5.2)$$

Using the conservation of probability ($P_0 + P_1 = 1$) we are left with

$$\dot{P}_0 = -\Gamma^T P_0 + \Gamma^- . \quad (5.3)$$

We consider now that the rate equations are modulated by two oscillating parameters, in our specific case V and n_g . We expand in power series of the amplitude of oscillation the rates keeping only the lowest orders:

$$\Gamma^\alpha(t) = \Gamma^{\alpha(0)}(t) + \Gamma^{\alpha(1)}(t) + \Gamma^{\alpha(2)}(t) + \dots \quad (5.4)$$

where α stands for any of the previously introduced labels, and the term into parenthesis indicates the order in the expansion. As far as the driving frequency is smaller than the temperature, $\hbar\omega_i \ll k_B T$, the explicit expression of the time-dependent rates can be obtained by that for the static case by substituting the time-dependent fields:[47] for instance

$$\Gamma^\alpha(t) = \Gamma^\alpha(a(t), b(t)), \quad (5.5)$$

where $a = a_0 + a_1(t)$, $b = b_0 + b_1(t)$, and $a_1(t) = a_1 \cos(\omega_1 t)$, $b_1(t) = b_1 \cos(\omega_2 t)$. One can then expand to second order in the time dependent part of the two parameters to obtain:

$$\begin{aligned} \Gamma^\alpha(t) = & \Gamma^\alpha + \frac{\partial \Gamma^\alpha}{\partial a} a_1(t) + \frac{\partial \Gamma^\alpha}{\partial b} b_1(t) + \frac{1}{2} \frac{\partial^2 \Gamma^\alpha}{\partial a^2} a_1^2(t) \\ & + \frac{\partial^2 \Gamma^\alpha}{\partial a \partial b} a_1(t) b_1(t) + \frac{1}{2} \frac{\partial^2 \Gamma^\alpha}{\partial b^2} b_1^2(t) + \dots \end{aligned}$$

The expansion up to second order can then be rearranged in a Fourier series:

$$\begin{aligned} \Gamma^\alpha(t) = & \Gamma_{00}^\alpha + \sum_{n=-1,1} \left[\Gamma_{n,0}^{\alpha(1)} e^{in\omega_1 t} + \Gamma_{0,n}^{\alpha(1)} e^{in\omega_2 t} \right] \\ & + \left[\Gamma_{1,-1}^{\alpha(2)} e^{i(\omega_1 - \omega_2)t} + \text{cc} \right] + \dots \end{aligned} \quad (5.6)$$

where the static part Γ_{00}^α has contributions of zero and second order in the driving fields. The notation $\Gamma_{n,m}^{\alpha(p)}$ indicates a contribution of order p in the driving intensity. Concerning the time dependent second order terms, we keep only the interesting part at the mixing-current frequency ω_Δ .

We look for a solution of the master equation in terms of the stationary Fourier components

$$P_0(t) = \sum_{n,m} A_{nm} e^{i(n\omega_1 + m\omega_2)t}. \quad (5.7)$$

This gives for each Fourier component the equation:

$$(in\omega_1 + im\omega_2)A_{nm} + \sum_{n',m'} \Gamma_{n'm'}^T A_{n-n',m-m'} - \Gamma_{nm}^- = 0. \quad (5.8)$$

We will solve the master equation through perturbation theory , expand the A and Γ^α in ϵ , with $\alpha = T, -$:

$$A_{nm} = \sum_{p=0}^{\infty} A_{nm}^{(p)} \epsilon^p, \quad (5.9)$$

$$\Gamma^\alpha = \sum_{n,m,q=0}^{\infty} \Gamma_{nm}^{\alpha(q)} \epsilon^q e^{i(n\omega_1+m\omega_2)t}, \quad (5.10)$$

where again q indicates the order in the driving fields, then the master equation becomes

$$\sum_{n,m} (in\omega_1 + im\omega_2) A_{n,m}^{(q)} + \sum_{n,m} \sum_{n',m',q'=0}^q \Gamma_{n',m'}^{T(q')} A_{n-n',m-m'}^{q-q'} = \sum_{n,m} \Gamma_{nm}^{-(q)}, \quad (5.11)$$

This leads to a set of equations that can be solved recursively. The detailed derivation for each order are as following:

For the zeroth-order ($q = 0$) one reads:

when $n = m = 0$, the last term zero order $\Gamma_{00}^{T(0)}$ exists only for $n' = m' = 0$,

$$\sum_{n',m'} \Gamma_{-n',-m'}^{T(0)} A_{-m',-n'}^{(0)} = \Gamma_{00}^{-(0)}. \quad (5.12)$$

this gives:

$$A_{00}^{(0)} = \frac{\Gamma_{00}^{-(0)}}{\Gamma_{00}^{T(0)}}. \quad (5.13)$$

For the first order:

when $n = m = 0, q = 1$,

$$\sum_{n',m'} \left[\Gamma_{n',m'}^{(0)} A_{-m',-n'}^{(1)} + \Gamma_{n',m'}^{(1)} A_{-m',-n'}^{(0)} \right] = 0, \quad (5.14)$$

this equation expands into more terms as following:

$$\Gamma_{0,0}^{(0)} A_{0,0}^{(1)} + \Gamma_{1,0}^{(1)} A_{-1,0}^{(0)} + \Gamma_{-1,0}^{(1)} A_{1,0}^{(0)} + \Gamma_{0,1}^{(0)} A_{0,0}^{(1)} + \Gamma_{0,0}^{(0)} A_{0,0}^{(1)} = 0, \quad (5.15)$$

when $n = 1, m = 0, q = 0$,

$$i\omega_1 A_{n0}^{(0)} + \sum_{n',m'} \Gamma_{n',m'}^{T(0)} A_{n-n',-m'}^{(0)} = \Gamma_{n,0}^{-(0)}, \quad (5.16)$$

the right term does not exist, then

$$i\omega_1 A_{10}^{(0)} + \sum_{n',m'} \Gamma_{n',m'}^{T(0)} A_{1,0}^{(0)} = 0, \quad (5.17)$$

then gives $A_{10}^0 = 0, A_{\pm 1,0}^0 = A_{0,\pm 1}^0 = 0$ can be obtained as the same way. Substituted these into Eq. (5.15), we obtain $A_{00}^{(1)} = 0$.

when $n, m = 0, q = 0$,

$$i\omega_1 A_{10}^{(0)} + \sum_{n',m'} \Gamma_{n',m'}^{T(0)} A_{-n',-m'}^{(0)} = \Gamma_{n,0}^{-(0)} = 0, \quad (5.18)$$

$$[ni\omega_1 + \Gamma_{00}^{T(0)}] A_{n,0}^0 = 0, \quad (5.19)$$

then

$$A_{n,0}^0 = A_{0,n}^0 = 0, \quad (5.20)$$

when $n = 1, m = 0, q = 1$,

$$i\omega_1 A_{10}^{(1)} + \sum_{n',m'} [\Gamma_{n',m'}^{T(0)} A_{-n',-m'}^{(0)} + \Gamma_{n',m'}^{T(1)} A_{1-n',1-m'}^0] = \Gamma_{10}^{-(1)}, \quad (5.21)$$

$$i\omega_1 A_{10}^{(0)} + \Gamma_{0,0}^{T(0)} A_{1,0}^{(1)} + \Gamma_{1,0}^{T(1)} A_{0,0}^{(1)} = \Gamma_{1,0}^{-(0)}, \quad (5.22)$$

$$[i\omega_1 + \Gamma_{0,0}^{T(0)}] A_{1,0}^{(1)} = \Gamma_{1,0}^{-(1)} - \Gamma_{1,0}^T A_{0,0}^{(0)}, \quad (5.23)$$

we obtain:

$$A_{1,0}^{(1)} = \frac{\Gamma_{0,1}^{-(1)} - \Gamma_{0,1}^T A_{0,0}^{(0)}}{+i\omega_1 + \Gamma_{0,0}^{T(0)}}, \quad (5.24)$$

the same for the other three terms $A_{-1,0}, A_{0,\pm 1}$, in the end we write the results under this case as following:

$$A_{0,\pm 1}^{(1)} = \frac{\Gamma_{\pm 1,0}^{-(1)} - \Gamma_{\pm 1,0}^T A_{0,0}^{(0)}}{\pm i\omega_2 + \Gamma_{0,0}^{T(0)}}, \quad (5.25)$$

$$A_{\pm 1,0}^{(1)} = \frac{\Gamma_{0,\pm 1}^{-(1)} - \Gamma_{0,\pm 1}^T A_{0,0}^{(0)}}{+ \pm i\omega_1 + \Gamma_{0,0}^{T(0)}}. \quad (5.26)$$

when $n = 1, m = -1, q = 1$,

$$i(\omega_1 - \omega_2)A_{1,-1}^1 + \sum_{n',m'} [\Gamma_{n',m'}^{T(0)} A_{1-n',1-m'}^1 + \Gamma_{n',m'}^{T(0)} A_{1-n',-1-m'}^{(0)}] = \Gamma_{1,-1}^{-(1)}, \quad (5.27)$$

$$[i(\omega_1 - \omega_2) + \Gamma_{00}^{T(0)}]A_{1,-1}^{(0)} = 0, \quad (5.28)$$

we obtain $A_{1,-1}^{(0)} = 0$.

when $n = 2, m = 0, q = 1$,

$$2\omega_1 A_{20}^{(1)} + \sum_{n',m'} [\Gamma_{n',m'}^{T(0)} A_{2-n',1-m'}^{(1)} + \Gamma_{n',m'}^{T(1)} A_{2-n',-m'}^{(0)}] = \Gamma_{20}^{-(1)}, \quad (5.29)$$

$$(n\omega_1 + \Gamma_{00}^{T(0)})A_{20}^{(1)} = \Gamma_{n0}^{-(1)}, \quad (5.30)$$

we obtain $A_{20}^1 = A_{02}^1 = 0$, this result can be same for $A_{n,0}^{(1)}, A_{0,n}^{(1)}$.

For the second order:

when $n, m, q = 2$,

$$[i(\omega_1 n - \omega_2 m)A_{n,m}^{(2)} + \sum_{n',m'} [\Gamma_{n',m'}^{T(0)} A_{n-n',m-m'}^{(2)} + \Gamma_{n',m'}^{T(1)} A_{n-n',m-m'}^{(1)} + \Gamma_{n',m'}^{T(2)} A_{n-n',m-m'}^{(0)}]] = \Gamma_{n,m}^{-(2)}, \quad (5.31)$$

here for this term $\Gamma_{n',m'}^{T(0)}$, need to be the zero order, only $\Gamma_{n',m'}^{T(0)}$ can be satisfied. Then this term becomes $\Gamma_{00}^{T(0)} A_{nm}^{(2)}$, for the term $\Gamma_{n',m'}^{T(1)} A_{n-n',m-m'}^{(1)}$, as $A_{00}^{(1)} = 0, A_{1,-1}^{(1)} = 0$, after been simplified, the term leaves $A_{\pm 1,0} \Gamma_{0,\pm 1}^{(0)}$. For $\Gamma_{n',m'}^{T(2)} A_{n-n',m-m'}^{(0)}$, as $A_{n,0}^{(0)} = 0$, we just keep the term $A_{00}^{(0)}$, then this term leaves $\Gamma_{n',m'}^{T(2)} A_{00}^{(0)}$.

Finally for the mixing term

$$A_{1,-1}^{(2)} = \frac{\Gamma_{1,-1}^{-(2)} - A_{00}^0 \Gamma_{1,-1}^{T(2)} - A_{1,0}^{(1)} \Gamma_{1,0}^{T(1)} - A_{0,-1}^{(1)} \Gamma_{1,0}^{T(1)}}{[i(\omega_1 - \omega_2) + \Gamma_{00}^{T(0)}]}. \quad (5.32)$$

The non-vanishing terms up to order two are $A_{0,0}^{(0)}$, $A_{\pm 1,0}^{(1)}$, $A_{0,\pm 1}^{(1)}$, $A_{0,0}^{(2)}$, $A_{\pm 2,0}^{(2)}$, $A_{\pm 1,\pm 1}^{(2)}$, and $A_{0,\pm 2}^{(2)}$. As usual for the Fourier transform of real functions the following relation holds: $A_{n,m}^* = A_{-n,-m}$.

Let us now consider the particle current. It can be expressed in terms of P and Γ , for instance, on the left junction (note that this expression does not include the displacement current):

$$I(t)/e = \Gamma^{L+} P_0 - \Gamma^{L-} P_1 = \Gamma^L P_0 - \Gamma^{L-}. \quad (5.33)$$

Substituting the expansion (5.7) into Eq. (5.33) we obtain for I a similar expansion to Eq. (5.7). The first three orders read:

$$I_{nm}^{(0)}/e = \left[\Gamma_{00}^{L(0)} A_{00}^{(0)} - \Gamma_{00}^{L-(0)} \right] \delta_{nm} \delta_{n0} \quad (5.34)$$

$$I_{nm}^{(1)}/e = \Gamma_{nm}^{L(1)} A_{00}^{(0)} + \Gamma_{00}^{L(0)} A_{nm}^{(1)} - \Gamma_{nm}^{L-(1)} \quad (5.35)$$

$$I_{nm}^{(2)}/e = \Gamma_{00}^{L(0)} A_{nm}^{(2)} + \sum_{n'm'} \Gamma_{n-n',m-m'}^{L(1)} A_{n'm'}^{(1)} + \Gamma_{nm}^{L(2)} A_{00}^{(0)} - \Gamma_{nm}^{L-(2)}. \quad (5.36)$$

The mixing current is given by

$$I_{\text{mx}}^c = \text{Re} I_{1,-1}/2 \quad , \quad I_{\text{mx}}^s = -\text{Im} I_{1,-1}/2. \quad (5.37)$$

In order to simplify the expressions obtained above we use the fact that in general $\omega_1 \approx \omega_2 \equiv \omega_D$ so that even in the fast oscillator limit $|\omega_1 - \omega_2| \ll \Gamma_{00}^{T(0)}$. This gives the approximate expressions:

$$A_{10}^{(1)} = \frac{\Gamma_{00}^T \Gamma_{10}^{-(1)} - \Gamma_{10}^{T(1)} \Gamma_{00}^{-(0)}}{\Gamma_{00}^{T(0)} (i\omega_D + \Gamma_{00}^{T(0)})} \quad (5.38)$$

$$A_{1,-1}^{(2)} = \frac{\Gamma_{1,-1}^{-(2)} - \Gamma_{1,0}^{T(1)} A_{0,-1}^{(1)} - \Gamma_{0,-1}^{T(1)} A_{1,0}^{(1)}}{\Gamma_{00}^{T(0)}} \quad (5.39)$$

One can see that the residual ω_D -dependence is due to the relaxation time of the charge in the island. As expected it disappears for $\omega_D \ll \Gamma_{00}^{T(0)}$. The contribution from $I_{1,-1}^{(1)}$ vanishes since $\Gamma_{1,-1}^{\alpha(1)} = 0$. The interesting part is the contribution of second order which reads:

$$I_{1,-1}^{(2)} = \Gamma_{00}^{L(0)} A_{1,-1}^{(2)} + \Gamma_{1,0}^{L(1)} A_{0,-1}^{(1)} + \Gamma_{0,-1}^{L(1)} A_{1,0}^{(1)} + \Gamma_{1,-1}^{L(2)} A_{00}^{(0)} - \Gamma_{1,-1}^{L-(2)}. \quad (5.40)$$

One can verify that for $\omega \ll \Gamma_{00}^{T(0)}$ expression Eq. (5.40) reduces to $\partial I^2 / \partial a \partial b$ recovering the standard results for the mixing-current [cf. expressions (3.11) and (3.10)].

In the opposite limit of $\omega \gg \Gamma_{00}^{T(0)}$ the first order correction to the charge variation vanishes ($A_{1,0}^{(1)} \rightarrow 0$): the charge has not the time to follow the driving. Only a second order correction survives $A_{1,-1}^{(2)} = \Gamma_{1,-1}^{-(2)} / \Gamma_{00}^{T(0)}$. The residual time dependence at the mixing frequency is only due to the direct modulation of the tunneling rates ($\Gamma_{1,-1}^{\alpha(2)}$). The final expression for $I_{1,-1}$ in the limit $\omega \rightarrow \infty$ reads:

$$I_{1,-1}^{(2)}_{\text{fast}} = \Gamma_{00}^{L(0)} \frac{\Gamma_{1,-1}^{-(2)}}{\Gamma_{00}^{T(0)}} + \Gamma_{1,-1}^{L(2)} A_{00}^{(0)} - \Gamma_{1,-1}^{L-(2)} \quad (5.41)$$

In the following chapter we consider explicitly the case of a metallic dot and of a single electronic level dot and we derive explicit expressions for the mixing current, its fluctuation and the response function in the high-frequency regime.

Chapter 6

Incoherent tunnelling regime

6.1 The metallic dot single-electron transistor

The expression for the tunnelling rate are well known for a metallic dot in the Coulomb blockade regime [39]. For convenience of the reader, we report in the Chapter 2 a very short derivation of the electrostatic relations. We consider only the two states with N and $N + 1$ electrons.

6.1.1 Low temperature case

We begin by discussing the low temperature case $k_B T \ll eV \ll E_C$ where $E_C = e^2/2C_\Sigma$ is the Coulomb energy. In this case there are only two non-vanishing rates (for $V > 0$)

$$\Gamma_L^+(N) = \Gamma_o(v + \tilde{n}_g)\theta(v + \tilde{n}_g) \quad (6.1)$$

$$\Gamma_R^-(N + 1) = \Gamma_o(v - \tilde{n}_g)\theta(v - \tilde{n}_g) \quad (6.2)$$

where $\Gamma_o = 1/RC_\Sigma$, $v = (C + C_g/2)V/e$ and $\tilde{n}_g = C_g(x)V_g/e - N - 1/2$, we assume a symmetric device with tunneling resistance R . The stationary solution to the master

equation (5.3) and the stationary current (5.33) read

$$P_1^{\text{st}} = \frac{\tilde{n}_g + v}{2v}, \quad I = e\Gamma_o \frac{v^2 - \tilde{n}_g^2}{2v}, \quad (6.3)$$

both equations valid for $|\tilde{n}_g| < v$. The current vanishes continuously for $|\tilde{n}_g| \geq v$ while the probability is 1 for $\tilde{n}_g > v$ and 0 for $\tilde{n}_g < -v$.

The driving amplitudes in terms of the dimensionless variables introduced read v_1 and n_{g1} . Note that the dependence of the rates on v and \tilde{n}_g is non-analytic for $\tilde{n}_g = \pm v$, this gives a constraint on the amplitude of the oscillations since the Taylor expansions are not valid if the parameters cross this values. This gives the constraints $|\tilde{n}_g \pm n_{g1}| < v$ and $v - v_1 > \tilde{n}_g$, that can be written $n_{g1}, v_1 < v - \tilde{n}_g$. Using Eq. (6.1) and Eq. (6.2) we can readily obtain the non-vanishing coefficients of the expansion (5.6):

$$\Gamma_{00}^{L+} = \Gamma_o(v + \tilde{n}_g), \Gamma_{10}^{L+} = \Gamma_o e^{i\varphi} n_{g1}/2, \Gamma_{01}^{L+} = \Gamma_o v_1/2, \quad (6.4)$$

$$\Gamma_{00}^{R-} = \Gamma_o(v - \tilde{n}_g), \Gamma_{10}^{R-} = -\Gamma_o e^{i\varphi} n_{g1}/2, \Gamma_{01}^{R-} = \Gamma_o v_1/2. \quad (6.5)$$

For $\omega_1 \approx \omega_2 = \omega_D$ we obtain a very simple expression for the component $I_{1,-1}$:

$$I_{1,-1} = e\Gamma_o \frac{\tilde{n}_g v_1 n_{g1} e^{-i\varphi}}{\tilde{\omega}_D^2 + 4v^2} \quad (6.6)$$

here we defined $\tilde{\omega}_D = \omega_D/\Gamma_o$. One finds thus a Lorentzian behaviour, the amplification factor decreases quite rapidly for large frequency driving ω_D . The main reason for the reduction of sensitivity is the incapacity of the charge in the dot to follow the driving signal. The crossover value for the frequency is $\omega_D \approx V/Re$, above this value one cannot use anymore the adiabatic approximation for the relaxation of the charge on the dot. It simply coincides with the frequency for which one electron per driving period crosses the device. For instance for $\omega_m = 100$ MHz, $R = 10^5$ Ohm, for voltage below a mV the corrections due to the retardation of the charge on the dot becomes relevant. This regime has been observed in the experiment presented in Ref. [48], where the crossover from slow to fast oscillator has been investigated by a fine tuning of the tunnelling resistances.

The amplification factor for the mechanical quadratures is thus:

$$\lambda = \frac{e\Gamma_o}{L} \frac{n_g \tilde{n}_g v_1}{(\tilde{\omega}_D^2 + 4v^2)}. \quad (6.7)$$

It is maximum for $\tilde{n}_g = \pm v$, but one should also take into account the constraint on the amplitude of $v_1 < v - |\tilde{n}_g|$. One way to take that into account is to set $v_1 = v - |\tilde{n}_g|$, this is the maximum allowed value for the driving amplitude, and since the signal increases linearly with v_1 , it gives the maximum value for λ . This gives:

$$\lambda = \frac{e\Gamma_o}{L} \frac{n_g \tilde{n}_g (v - |\tilde{n}_g|)}{(\tilde{\omega}_D^2 + 4v^2)}. \quad (6.8)$$

The maximum of λ as a function of the gate voltage is obtained for $\tilde{n}_g = \pm v/2$ and its value (for $\tilde{\omega}_D \ll v$) is

$$\lambda = \frac{e\Gamma_o n_g}{16L} \quad (6.9)$$

independently of v . For a typical device one has $n_g \approx 100$, $L \approx 1\mu\text{m}$, $\Gamma_0 = 10^{11}$ Hz leading to $\lambda \sim 0.1$ A/m [9, 10].

The gain is only a part of the detection, one has also to evaluate the noise. For that we need the two contributions considered in the Chapter 4.

Shot noise. The Fano factor has been obtained in Ref. [40] (cf. Eq. 41 there):

$$\mathcal{F} = \frac{\Gamma_L^{+2} + \Gamma_R^{-2}}{(\Gamma_L^+ + \Gamma_R^-)^2} = \frac{v^2 + \tilde{n}_g^2}{2v^2} \quad (6.10)$$

it varies between 1/2 and 1. The shot noise becomes thus:

$$S_{II}^{\text{shot}} = e^2 \Gamma_o \frac{v^4 - \tilde{n}_g^4}{2v^3}. \quad (6.11)$$

Charge noise. To obtain the contribution of the displacement fluctuation we need to calculate the charge noise correlation function:

$$S_n(t) = \langle \delta n(t) \delta n(0) \rangle, \quad (6.12)$$

where $\delta n = n - \langle n \rangle$ is the fluctuation of the charge, $\langle n \rangle$ is the average of the charge. First we calculate the correlation function of the charge:

$$\langle n(t)n(0) \rangle = \sum_{n_1, n_2} P(n_1, t | n_2, 0) P_1^{st} = P(1, t | 1, 0) P_1^{st} \quad (6.13)$$

where the conditional probability $P(1, t | 1, 0)$ that it was occupied at time $t > 0$ with the condition that it was occupied at time 0 can be obtained by solving the master equation

$$P(1t | 10) = P_1(t) = e^{-\int_0^t \Gamma_T dt'} \left(\int \Gamma_L e^{\int_0^t \Gamma_T dt'} dt + C \right) \quad (6.14)$$

with initial condition for $t = 0, P_1 = 1$, then $C = \Gamma_R/\Gamma_T$

$$P_1 = (\Gamma_R/\Gamma_T)e^{-\Gamma_T t} + \frac{\Gamma_L}{\Gamma_T} \quad (6.15)$$

$P_{st} = \Gamma_+/\Gamma_T$ is the stationary solution that is realized for $t \gg 1/\Gamma_T$, then correlation function of the charge:

$$\langle n(t)n(0) \rangle = \frac{\Gamma_L \Gamma_R}{\Gamma^2} e^{-\Gamma_T t} + \left(\frac{\Gamma_L}{\Gamma_T} \right)^2 \quad (6.16)$$

As Charge noise can be expressed as following:

$$\langle \delta n(t) \delta n(0) \rangle = \langle n(t)n(0) \rangle - \langle n(t) \rangle \langle n(0) \rangle \quad (6.17)$$

then the charge noise can be obtained by Fourier transform:

$$S_n(\omega) = P_1^{st} (1 - P_1^{st}) \frac{2\Gamma^T}{\omega^2 + \Gamma^T} \quad (6.18)$$

As expected the correlation function is flat for $\omega \ll \Gamma^T$, the required low frequency correlator reads then:

$$S_n(\omega = 0) = 2\Gamma^+ \Gamma^- / (\Gamma^T)^3. \quad (6.19)$$

In the specific case of low temperature one obtains thus $S_n = (v^2 - \tilde{n}_g^2)/(4\Gamma_o v^3)$.

In the typical working regime of a SET $V \ll V_g$, and $n_g \approx N$. Using the Eq. (2.1) one finds that $Q_g/e \approx n_g \approx N$. We thus have $F_0 = 2NE_C/L$. Collecting all the terms we can

substitute into Eq. (4.18) to obtain:

$$S_I^{\text{ba}} = 2e^2\Gamma_o N^4 \left(\frac{E_c}{kL^2} \right)^2 \frac{(v^2 - \tilde{n}_g^2)\tilde{n}_g^2}{v^5}. \quad (6.20)$$

The ratio of the mechanical to the shot noise is thus:

$$\frac{S_I^{\text{ba}}}{S_I^{\text{shot}}} = \left(\frac{E_c}{kL^2} \right)^2 \frac{4N^4\tilde{n}_g^2}{v^2(v^2 + \tilde{n}_g^2)}. \quad (6.21)$$

For large mechanical coupling (L small and N large) the mechanical noise dominate for $1 \gg \tilde{n}_g \gg kL^2v^2/(2E_cN^2)$. At small values of \tilde{n}_g the shot noise always dominates due to the vanishing of the gain ($\partial I/\partial n_g \rightarrow 0$).

From Eqs (6.9), (6.11), and (6.20), we obtain the seeked added noise as defined by Eq. (4.19). In order to study its dependence on the different parameters it is convenient to introduce the two dimensionless variables $\nu \equiv \tilde{n}_g/v$ and the dimensionless coupling constant $\delta \equiv (E_c/kL^2)(N^2/v) = \epsilon_P/eV$, where $\epsilon_P = F_0^2/k$ is the energy scale of the electromechanical coupling [13, 14, 18]. The added noise then reads:

$$S_x^{\text{add}} = \frac{E_c}{k\Gamma_0} f(\nu, \delta), \quad (6.22)$$

with

$$f(\nu, \delta) = \frac{2(1 + \nu)[4(\delta^2 + 1)\nu^2 + 1]}{\nu^2(1 - \nu)\delta}, \quad (6.23)$$

and $0 < \nu < 1$. The function diverges for $\nu \rightarrow 1$ due to the fact that we have to limit the amplitude of the voltage modulation and diverges for $\nu \rightarrow 0$ due to the vanishing of the amplification factor. The minimum added noise is thus always for values of ν between 0 and 1. In the weak coupling limit, for $\delta \ll 1$, one finds that the minimum is at $\nu \approx 0.54$ and reads

$$S_x^{\text{add}} \approx 14.8 \frac{E_c/k}{\Gamma_0} \frac{eV}{\epsilon_P}. \quad (6.24)$$

For strong coupling, $\delta \gg 1$, instead the minimum is close to $\nu = 0$ with a value for

$$S_x^{\text{add}} \approx 8 \frac{E_c}{k\Gamma_0} \left(\frac{\epsilon_P}{eV} \right)^2. \quad (6.25)$$

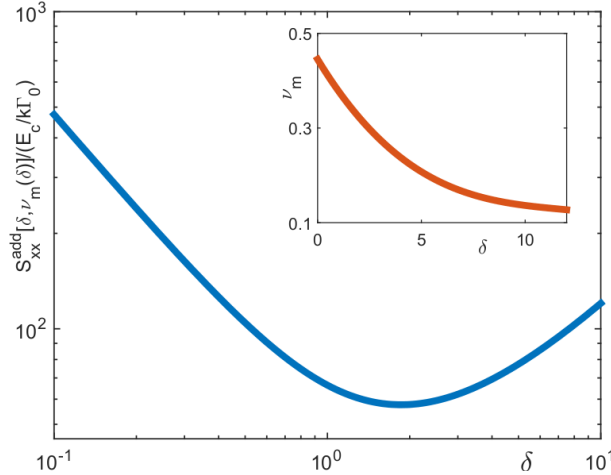


FIGURE 6.1: S_{xx}^{add} as a function of $\delta = \epsilon_P/eV$ for $\nu(\delta)$ minimizing the function. In a inset the value of ν that minimizes the function for given δ [$\nu_m(\delta)$].

In both cases the noise diverges when δ becomes very small or very large. In the weak coupling limit the added noise is dominated by the current noise (imprecision noise), in the strong coupling it is instead given essentially by the back-action noise. As usual [46] the optimal situation is in the middle for $\delta \approx 1$.

In Fig. 6.1 we plot $S_x^{\text{add}}[\delta, \nu_m(\delta)]$, where $\nu_m(\delta)$ is the value of ν that minimizes S_x^{add} for given δ . We thus find that the absolute minimum for the added noise is obtained for $\nu = 0.32$ and $\delta = 1.857$ and reads

$$S_{xx}^{\text{add}} = 57.61 \frac{E_c}{k\Gamma_0} \quad (6.26)$$

This is the ultimate sensitivity that can be obtained with this device in ideal conditions, when all other sources of imprecisions have been eliminated. Inserting typical values of $E_c \approx 10K$, $\Gamma_0 \approx 10^{11}Hz$, $k = 10^{-5}N/m$ one obtains the value of $S_{xx}^{\text{add}} \approx 10^{-26}m^2/Hz$. One should regard this value with some caution. Let's consider the value of the coupling that is required to obtain this sensitivity. The optimal value of δ is for $eV \approx \epsilon_P$. As discussed in the literature (see for instance Ref. [18], where this energy is called E_E) this scale determines the value at which the system undergoes a current blockade. It is difficult to reach this limit (since one needs also $k_B T \ll \epsilon_P$) in metallic SETs. On the other side ϵ_P of the order of 0.3 K has been observed in suspended carbon nanotubes [48]. The dramatic effects expected at low temperature on the mechanical resonators have been discussed recently [26, 27]. This extreme limit need to be reconsidered, since

the resonating frequency of the resonator is renormalized by the coupling, and the added noise induced by the oscillator is expected to be more effective. In particular the oscillator becomes strongly non-linear close to the transition.

We can estimate in a simple way the effect of the softening of the mechanical resonator following Ref. [18]. The correction to the variation of the energy reads [11]:

$$\Delta E^\pm \rightarrow \Delta E^\pm \pm F_0 x \quad (6.27)$$

this changes the form of P_1^{st} given by Eq. (6.3) as follows:

$$P_1^{\text{st}} = \frac{\tilde{n}_g + xF_0/(2E_C) + v}{2v}. \quad (6.28)$$

Substituting into the equation for the average force $F_0 P_{\text{st}}^1$ and taking the derivative with respect to x one obtains the renormalized spring constant:

$$k' = k(1 - \delta). \quad (6.29)$$

The instability appears for $\delta = 1$, where two new stable solutions bifurcate. The only change in our previous calculations is the value of k entering Eq. (4.19):

$$S_{xx}^{\text{add}} = \frac{E_c}{k\Gamma_0} \frac{1}{1 - \delta} f[\nu, \delta/(1 - \delta)]. \quad (6.30)$$

Repeating the minimization procedure we find that the minimum is now for $\delta = 0.48$ holding the value of $132.7(E_c/k\Gamma_0)$. Thus the renormalization of the resonating frequency reduces the precision of a factor of 2, leaving space for high sensitivity detection.

The actual limitation in current experiments will be the value of the coupling, since in practice the typical temperature reached in experiments on metallic quantum dot is much larger than ϵ_P . In the following section we consider the detection at finite temperature and low voltage.

6.1.2 Finite temperature case

Let us now consider the finite temperature case $eV \ll k_B T \ll E_C$. In this case we have to take into account the four possible tunnelling processes that change the charge on the dot from the N to the $N + 1$ state (Chapter 2). The respective rates read:

$$\Gamma_{L(R)}^+(N) = \Gamma_{\text{Th}} h[(\mp eV - 2\tilde{n}_g E_C)/k_B T], \quad (6.31)$$

$$\Gamma_{L(R)}^+(N + 1) = \Gamma_{\text{Th}} h[(\pm eV + 2\tilde{n}_g E_C)/k_B T], \quad (6.32)$$

with $h(y) = -y[1 - e^y]$ and $\Gamma_{\text{Th}} = k_B T/e^2 R$. We consider the low bias voltage limit $eV/k_B T \ll 1$. In this limit the expression for the current Eq. (5.33) becomes:

$$I = e\Gamma_{\text{Th}} \frac{eV}{2k_B T} g(2\tilde{n}_g E_C/k_B T), \quad (6.33)$$

where

$$g(y) = \frac{h_+ h'_- + h'_+ h_-}{h_+ + h_-} = \frac{e^y y}{e^{2y} - 1} \quad (6.34)$$

and $h_{\pm} = h(\pm y)$. From the expression of the current we obtain

$$\frac{\partial^2 I}{\partial V \partial \tilde{n}_g} = -\frac{E_C}{Rk_B T} g'(2\tilde{n}_g E_C/k_B T), \quad (6.35)$$

(for brevity, we omit in the following the arguments of g and of the other functions of $y = 2\tilde{n}_g E_C/k_B T$) with the amplification factor:

$$\lambda = \frac{n_{g0} \Gamma_0 e V_1}{4Lk_B T} g' \approx \frac{F_0 V_1}{8Rk_B T} g'. \quad (6.36)$$

The factor $g'(x)$ has a maximum for $y = 1.16$ for which it holds the approximate value 0.154. Thus tuning $\tilde{n}_g = 0.58k_B T/E_C$ allows to obtain the maximum value of the amplification factor. Comparing this value to Eq. (6.9), valid for $k_B T \ll eV$, we see that the amplification factor is reduced by the term $eV_1/k_B T \ll 1$.

The shot noise at low frequency reads [40]:

$$S_I^{\text{shot}} = e^2 \left[\frac{\Gamma_L^+ \Gamma_R^- + \Gamma_L^- \Gamma_R^+}{\Gamma_T} - 2 \frac{(\Gamma_L^+ \Gamma_R^- - \Gamma_L^- \Gamma_R^+)^2}{\Gamma_T^3} \right]. \quad (6.37)$$

For small V the first term (thermal noise) dominates and gives:

$$S_I^{\text{shot}} = e^2 \Gamma_{\text{Th}} \frac{h_+ h_-}{h_+ + h_-}. \quad (6.38)$$

The charge noise in the same limit reads

$$S_n = \frac{1}{\Gamma_{\text{Th}}} \frac{h_+ h_-}{(h_+ + h_-)^3}. \quad (6.39)$$

From the expression of the back-action noise (4.18) we see that for $V \rightarrow 0$ there is (apparently) no back action of the measurement. It is possible to set $V = 0$ and exploit its modulation around 0 to detect the motion of the oscillator. But in this case we need to consider the next order in the expansion (3.8). For $V = 0$ we have:

$$\delta I = \frac{\partial I}{\partial n_g \partial V} \delta n_g V_1 + \dots \quad (6.40)$$

From this we have for the current-current correlator:

$$\langle \delta I(t_1) \delta I(t_2) \rangle = \left(\frac{\partial G}{\partial n_g} \right)^2 V_1(t_1) V_1(t_2) \langle \delta n_g(t_1) \delta n_g(t_2) \rangle, \quad (6.41)$$

where $G = dI/dV$ for $V = 0$ is the conductance. The product of the two V_1 terms gives an oscillating term depending on $t_1 + t_2$ that averages to zero and a second term proportional to $\cos[\omega_2(t_1 - t_2)]$. Using $\delta n_g(t) = (C'_g V_g / e) \delta x(t)$ we have

$$S_I^{\text{ba}} = \frac{1}{2} \left(\frac{\partial G}{\partial n_g} \right)^2 (V_{g0} C'_g V_1 / e)^2 S_x(\omega_2). \quad (6.42)$$

Typically $\omega_2 \approx \omega_m$, we thus assume that it is resonant in order to evaluate the case of maximal back-action:

$$S_I^{\text{ba}} = \frac{g'^2 h_+ h_-}{16(h_+ + h_-)^3} e^2 \Gamma_0 \frac{\epsilon_P^2 Q^2 (eV_1)^2}{(k_B T)^3 E_C}, \quad (6.43)$$

with $h^{\text{ba}} = (g')^2 h_+ h_- / (h_+ + h_-)^3$ and $Q = \omega_m / \gamma$ the oscillator quality factor.

Adding the two sources of current noise Eq. (6.43) and Eq. (6.38) we obtain for the added noise:

$$S_x^{\text{add}} = \frac{E_C}{k\Gamma_0} \left[\alpha^{\text{ba}} \frac{\epsilon_P Q^2}{k_B T} + \alpha^{\text{shot}} \frac{(k_B T)^3}{\epsilon_P (eV_1)^2} \right], \quad (6.44)$$

with the numerical factors $\alpha^{\text{ba}} = 4h_+h_-/(h_+ + h_-)^3$ and $\alpha^{\text{shot}} = 32h_+h_-/[(g')^2(h_+ + h_-)]$. Choosing the value $\tilde{n}_g = 1.60$ that maximizes λ their values are $\alpha^{\text{ba}} = 0.23$ and $\alpha^{\text{shot}} = 449$.

The minimum of the added noise is obtained for

$$\epsilon_P = \left(\frac{\alpha^{\text{shot}}}{\alpha^{\text{ba}}} \right)^{1/2} \frac{(k_B T)^2}{Q e V_1}, \quad (6.45)$$

with a minimum noise of

$$S_x^{\text{add}} = 2 \frac{E_C}{k\Gamma_0} (\alpha^{\text{ba}} \alpha^{\text{shot}})^{1/2} Q \frac{k_B T}{e V_1}. \quad (6.46)$$

Since $eV_1/k_B T \ll 1$, at best we can set this ratio to 0.1. This gives for the optimal value of the coupling

$$\frac{\epsilon_P}{k_B T} \approx \frac{441}{Q} \quad (6.47)$$

and the minimum of the added noise

$$S_x^{\text{add}} = 203 \frac{Q E_C}{k\Gamma_0}. \quad (6.48)$$

Some comments are at order. First we assumed that the frequency driving the voltage bias is resonant with the oscillator. This is an upper limit to the back action, in particular if $Q \gg 1$ this condition is not fulfilled and the back action will be reduced. For the non-resonant case it is sufficient to use the above results with $Q \approx \omega_m/\omega_\Delta$, reducing enormously the minimum added noise, to the expenses of finding a much larger coupling constant. The limitation is given essentially by the band-width of the device, $|\omega_1 - \omega_2|$ should be as large as possible (in particular larger than ω_m/Q), but yet smaller than the band width. The second comment concern the value of the coupling constant ϵ_P necessary to reach the minimum. One can see that even with the assumption of resonant back action it is relatively large. For a typical $Q \approx 10^4$ one finds $\epsilon_P/k_B T \approx 0.04$. To

our knowledge the largest value of the ratio $k_B T / \epsilon_P$ is ≈ 0.017 has been reported in Ref. [48]. Since as soon as $Q \gg 1$ it is possible to avoid resonant back-action, in most cases the main limitation is to reach large values of ϵ_P .

It is interesting to compare the shot-noise contribution of the added noise with the resonant brownian motion fluctuations:

$$S_x^B(\omega_m) = 2 \frac{k_B T}{k\gamma}. \quad (6.49)$$

The ratio reads:

$$\frac{S_x^{\text{add}}}{S_x^B} = \frac{\alpha^{\text{shot}}}{2} \frac{E_C \gamma}{\epsilon_P \Gamma_0} \left(\frac{k_B T}{eV_1} \right)^2. \quad (6.50)$$

Detection of brownian motion can then be done for $\epsilon_P / E_C > 2 \times 10^4 \gamma / \Gamma_0$ (where we assumed as before $eV_1 / k_B T = 0.1$). For instance in Ref. [10] $\gamma / \Gamma_0 \approx 10^{-8}$ allowing the detection of the brownian motion fluctuations even for very weak coupling. For a rough estimate of the coupling in that experiment one can use the expression given in Ref. [26] $\epsilon_P / k_B T \approx 2\delta\omega_m / \omega_m$, where $\delta\omega_m$ is the modulation of the resonating frequency near the degeneracy point (see Fig. 3 in Ref. [10]). For Ref. [10] one finds $\epsilon_P \approx 16$ mK to be compared to E_C of the order of 10K. Notwithstanding the low value of the coupling constant, the resolution is largely sufficient to detect the Brownian motion of the carbon nanotube.

6.2 The single-electronic level SET

When the temperature and the voltage bias is much smaller than the electronic level separation the rates for electron transfer reads [49]:

$$\Gamma_{L(R)}^+ = \Gamma_{L(R)0} f_F[(\epsilon - \mu_{L(R)}) / k_B T], \quad (6.51)$$

$$\Gamma_{L(R)}^- = \Gamma_{L(R)0} [1 - f_F[(\epsilon - \mu_{L(R)}) / k_B T]], \quad (6.52)$$

where $f_F(y) = 1 / (1 + e^y)$ is the Fermi function, ϵ is the level position, $\mu_L(R)$ is the left (right) chemical potential, and $\Gamma_{L(R)0}$ are the transfer rates. This regime can be realised

for instance to suspended carbon nanotubes where quantum dot forms. For simplicity in the following we choose $\Gamma_{L0} = \Gamma_{R0} = \Gamma_0$. The modulation of the gate voltage leads to the time-dependence $\epsilon(t) = \epsilon_0 + \epsilon_1(t)$ of the electronic level energy ϵ with

$$\epsilon_0 = \epsilon_{d0} + eC_g V_{g0}/C_\Sigma, \quad (6.53)$$

$$\epsilon_1(t) = e[C'_g V_{g0} x(t) + C_g V_{g1}(t)]/C_\Sigma, \quad (6.54)$$

and ϵ_{d0} the position of the electronic level for vanishing V_g . We assume symmetric bias so that the chemical potential read:

$$\mu_{L(R)}(t) = \mu_{L(R)0} + (-)e(V + V_1 \cos \omega_2 t)/2. \quad (6.55)$$

Following the steps of the previous section we can calculate the current

$$I = \frac{e\Gamma_0}{2} [f_F[(\epsilon - \mu_L)/k_B T] - f_F[(\epsilon - \mu_R)/k_B T]] \quad (6.56)$$

from which we obtain for vanishing V the amplification factor:

$$\lambda = \frac{en_{g0}\Gamma_0}{4L} \frac{eV_1 E_C}{(k_B T)^2} f_F''(y), \quad (6.57)$$

where the argument of the Fermi function is $y = (\epsilon_0 - \mu)/k_B T$, and will be omitted in the following. The maximum of f_F'' is obtained for $y = 1.31$ with a value of 0.096. The thermal part of the shot noise and the charge noise read:

$$S_I^{\text{shot}} = e^2 \Gamma_0 f_F(1 - f_F), \quad (6.58)$$

$$S_n = \frac{f_F(1 - f_F)}{\Gamma_0}. \quad (6.59)$$

Using Eq. (6.42) for the back-action noise we obtain

$$S_I^{\text{ba}} = \frac{f_F(1 - f_F)f_F''^2}{8} e^2 \Gamma_0 \left(\frac{eV_1 Q \epsilon_P}{(k_B T)^2} \right)^2. \quad (6.60)$$

The added noise has thus the form:

$$S_x^{\text{add}} = \frac{k_B T}{k\Gamma_0} \left[\alpha^{\text{ba}} Q^2 \frac{\epsilon_P}{k_B T} + \alpha^{\text{shot}} \left(\frac{k_B T}{eV_1} \right)^2 \frac{k_B T}{\epsilon_P} \right] \quad (6.61)$$

with $\alpha^{\text{ba}} = 2f_F(1 - f_F)$ and $\alpha^{\text{shot}} = 16f_F(1 - f_F)/f_F''^2$. Their values for $y = 1.31$ are $\alpha^{\text{ba}} = 0.34$ and $\alpha^{\text{shot}} = 289.2$. We find the same value of ϵ_P for the minimum of the added noise in the metallic case [cf. Eq. (6.45)], but the minimum of the noise has a different expression:

$$S_x^{\text{add}} = 2 (\alpha^{\text{ba}} \alpha^{\text{shot}})^{1/2} \frac{(k_B T)^2}{k\Gamma_0 eV_1}. \quad (6.62)$$

Essentially the energy scale of the Coulomb blockade is substituted by the temperature, in principle reducing the added noise. The conclusion is that the single-level SET should allow a better resolution of the metallic SET by a factor $E_C/k_B T$.

Chapter 7

Coherent tunnelling regime

In this chapter we consider the sensitivity of the device when the electronic transport is realized in the coherent regime. We will model the electronic system as in Ref. [26], that is relevant for the description of recent experiments [48, 50]. This system has been shown to be particularly interesting in the strong coupling limit [26, 27]. Defining like in the previous chapters F_0 the additional force acting on the oscillator when an electron is added to the suspended island and k the mechanical spring constant, it has been shown in Ref. [26] that the system undergoes a mechanical bistability at $\epsilon_P = F_0^2/k = \pi\Gamma$ with an expected universal quality factor Q of the order of 1.71. Since the previous chapters we found that best sensitivities are obtained for large values of the coupling constant it is interesting to consider this model and study the condition for an optimal detection of the oscillation amplitude with the current-mixing technique. The main question is how the bistability and the unusual fluctuations of the oscillator may influence the sensitivity. We will find that in most cases increasing the coupling allows to reach a better sensitivity, and thus the ultimate limit is the onset of the bistability. Once in the bistable regime both the progressive reduction of the current due to the establishment of the current blockade and a strong telegraph noise due to the hopping between the two stable minima reduce the efficacy of the detection device.

7.1 Model

We consider electronic transport through a single electronic level quantum dot capacitively coupled to a mechanical oscillator, as is the case, for instance, in state of the art experiments with carbon nanotubes [48]. The system can be described by the following Hamiltonian:

$$H = H_L + H_R + H_T + \epsilon_d(x)d^\dagger d + \frac{p^2}{2m} + \frac{kx^2}{2}. \quad (7.1)$$

The first three terms describe the leads and their coupling to the electronic level: $H_\alpha = \sum_k (\epsilon_{\alpha k} - \mu_\alpha) c_{\alpha k}^\dagger c_{\alpha k}$ with $\alpha = L(R)$ for the left (right) lead, $H_T = \sum_k t_{\alpha k} c_{\alpha k}^\dagger d$, with c and $\epsilon_{\alpha k}$ the destruction operator and the energy of the electrons in the leads, respectively, and μ_α the chemical potential. From these quantities one can define the lead's tunneling rate $\Gamma_\alpha = \pi t_{\alpha}^2 \rho_\alpha$ with ρ_α the density of the states and the single-level width $\Gamma = \Gamma_L + \Gamma_R$. For simplicity in the following we choose $\Gamma/2 = \Gamma_L = \Gamma_R$. The last two terms of Eq. (7.1) describe a single mechanical mode of displacement x , momentum p , mass m , and resonating frequency $\omega_0^2 = k/m$. The coupling between the electronic and the mechanical degrees of freedom is encoded in the fourth term, that gives the energy of the single electronic level $\epsilon_d(x)$. In order to find the gate voltage dependence of the energy level we simply calculate the difference in the electrostatic energy and electronic energy when one electron is added to a quantum dot where a charge Q is already present:

$$\Delta E = E(Q - e) - E(Q). \quad (7.2)$$

Using the expressions for the electrostatic energy (cf. Chapter 2) one finds

$$\Delta E = \frac{(Q - e)^2}{2C_\Sigma} - \frac{Q^2}{2C_\Sigma} - e \sum_{i=L,R,g} V_i C_i + \epsilon_{d0}, \quad (7.3)$$

with V_L , V_R , and V_g the voltage applied to the left, right, and gate electrode. The first two terms represent the contribution of the local electrostatic energy, the third one is the contribution of the sources, and the last one is the electronic level energy. (We consider spinless electrons.) In order to reach the strong coupling regime one will typically work

in the limit of $Q \gg e$. Moreover for the same reasons typically $V_L - V_R = V \ll V_g$. With these approximations one obtains:

$$\epsilon_d(x) = \epsilon_{d0} - eC_g(x)V_g/C_\Sigma. \quad (7.4)$$

It depends on the displacement of the oscillator, that we assume coupled to the electronic level through the modulation of a gate capacitance $C_g(x)$. The variation of the force acting on the oscillator can be obtained by calculating the derivative of ΔE :

$$F_0 = -\frac{\partial \Delta E}{x} = e \frac{C'_g}{C_\Sigma} \left(V_g + \frac{e}{2C_\Sigma} - \frac{\sum_i V_i C_i + Q}{C_\Sigma} \right). \quad (7.5)$$

In the usual regime $Q \gg e$, $V \ll V_g$, and $Q = -eN \approx -C_g V_g$ one obtains

$$F_0 = e \frac{C'_g}{C_\Sigma} V_g \approx \frac{2NE_C}{L} \quad (7.6)$$

where $E_C = e^2/2C_\Sigma$ is the Coulomb energy and $L = C_g/C'_g$ is the length scale of the induced coupling. We defined as previously $C_\Sigma = C_L + C_R + C_g$ the sum of the three capacitances associated to the three leads (see Fig. 3.1). The bias voltage satisfies the relation $V = (\mu_R - \mu_L)/e$.

We will work in the typical regime of most experiments: $\omega_m \ll \Gamma$ and $\omega_m \ll eV$ or $k_B T$. This allows to use Born-Oppeneimer approximation and to treat the mechanical mode as a classical degree of freedom [16, 19]. By expanding the x -dependence we obtain:

$$\epsilon_d(x) = \epsilon_0 - F_0 x, \quad (7.7)$$

where $\epsilon_0 = \epsilon_{d0} - eC_g(0)V_g/C_\Sigma$ and $F_0 = eC'_g(0)V_g/C_\Sigma$.

In a previous Chapter 6, we considered the sensitivity of this detection device in the incoherent tunnelling regime: $k_B T \gg \Gamma$. In the present chapter we consider the opposite case of coherent tunnelling regime $k_B T \ll \Gamma$. For the description of the dynamics of the device we follow Ref. [26, 27]. Since the oscillator is slow one can calculate the

position-dependent current for given value of x [27]:

$$I(x) = e^2 \int \frac{d\omega}{2\pi} \tau(z_\omega) [f_L(\omega) - f_R(\omega)], \quad (7.8)$$

where

$$\tau(z) = \frac{1}{1 + z^2} \quad (7.9)$$

is the energy dependent electronic transmission factor through the quantum dot, $z_\omega = (\omega - \epsilon_0 + F_0 x)/\Gamma$, and $f_\alpha(\omega) = (1 + e^{(\omega - \mu_\alpha)/T})^{-1}$ is the lead α Fermi distribution. This expression depends on the position of the oscillator, and in order to obtain the measured value one should average over the positions of the oscillator over its statistical distribution. We are interested in the low voltage limit $eV \ll k_B T$. In this case τ is a smooth function of ω with respect to the Fermi distributions and we can approximate $f_L(\omega) - f_R(\omega) = \delta(\omega - \mu)eV$, where for $V \rightarrow 0$ we defined $\mu = \mu_L = \mu_R$. Eq. (7.8) simplifies to

$$I = \frac{e^2 V}{2\pi} \tau(z_x), \quad (7.10)$$

where

$$z_x = (\mu - \epsilon_0 + F_0 x)/\Gamma. \quad (7.11)$$

The displacement dynamics of the mechanical mode can be described by a Langevin equation:

$$m[\ddot{x} + \gamma(x)\dot{x} + \omega_0^2 x] = \xi(t) + F_e(x). \quad (7.12)$$

In Eq. (7.12) the quantity $F_e(x) \equiv F_0 n_d(\epsilon_0 - F_0 x)$ is the average force acting on the oscillator. It is simply proportional to the average occupation of the dot $n_d \equiv \langle d^\dagger d \rangle$. The fluctuating part of the force generated by the electrons jumping in and out the dot is modeled by the stochastic force $\xi(t)$ that is assumed to have gaussian fluctuations with $\langle \xi(t)\xi(t') \rangle = D(x)\delta(t - t')$ on a time scale longer than Γ^{-1} . Also originating from the fluctuation of the charge on the dot $\gamma(x)$ is the dissipative coefficient. Both γ and D can be related to the spectrum of charge fluctuation on the dot $S_{nn}(t) = \langle n_d(t)n_d(0) \rangle$: $D(x) = F_0^2 S_{nn}(x, \omega = 0)$, $\gamma(x) = -(F_0^2/m)(\partial S_{nn}/\partial \omega)(x, \omega) |_{\omega=0}$, The explicit expressions

for γ , F_e and D are given in Ref. [27] :

$$\langle n_d \rangle = \int_{-\infty}^{\infty} \frac{d\omega}{2\pi\Gamma} (f_L + f_R)\tau, \quad (7.13)$$

$$S_{nn}|_{\omega=0} = \sum_{\alpha,\beta} \int_{-\infty}^{+\infty} \frac{d\omega}{2\pi\Gamma^2} f_\alpha (1 - f_\beta) \tau^2, \quad (7.14)$$

and

$$\left. \frac{dS_{nn}}{d\omega} \right|_{\omega=0} = \sum_{\alpha,\beta} \int_{-\infty}^{+\infty} \frac{d\omega}{2\pi\Gamma^2} f_\alpha \tau [f'_\beta \tau - (1 - f_\beta) \tau']. \quad (7.15)$$

From Eq. (7.12) one can derive a Fokker-Planck equation for the probability distribution $P(x, p, t)$ that the oscillator is at position x with momentum p at time t :

$$\partial_t P = \frac{p}{m} \partial_x P - F \partial_p P + \gamma \partial_p (pP) + \frac{D}{2} \partial_p^2 (P) \quad (7.16)$$

where $F(x) = -kx + F_e(x)$.

7.2 Current noise sources

We consider now the two contributions to the current noise sources.

7.2.1 Intrinsic electronic current noise

The current fluctuates due to the discrete nature of the charge and due to the thermal fluctuations. For simplicity and coherence with the notation of Ref. [52], we use the notation S_I^{shot} , even if in practice in the following we will consider only the case of dominant thermal fluctuations. For a single channel two-terminal conductor the noise power spectrum ($S_I(\omega) = 2 \int dt e^{i\omega t} \langle I(t)I(0) \rangle$) of the current fluctuations for $V, k_B T \ll \Gamma$ reads [51]:

$$S_I^{\text{shot}} = \frac{e^2}{\pi} \left[2k_B T \tau^2 + eV \coth \left(\frac{eV}{2k_B T} \right) \tau(1 - \tau) \right], \quad (7.17)$$

where the first term is the equilibrium noise contribution and the second term is the non-equilibrium or shot noise contribution to the power spectrum. In the regime of interest

for most experiments in nanomechanical systems, $eV \ll k_B T$, we are left with

$$S_I^{\text{shot}}(\omega) = \frac{2k_B T e^2}{\pi} \tau(z). \quad (7.18)$$

Here z should be averaged over $P(x, p, t)$, but for weak coupling the probability has a sharp peak at the equilibrium position x_e of the oscillator, and one can simply use this value of x in the definition of $z = z_e$.

7.2.2 Back-action current noise

The coupling of the mechanical oscillator to the electronic detector induces fluctuations even in the quasi-equilibrium limit of $eV \ll k_B T$. The fluctuation of the charge on the quantum dot induces a stochastic force that put the oscillator into motion. The displacement of the oscillator affects the effective energy level position, through Eq. (7.7), that in turn generates fluctuations of the current that induces fluctuation of the mixing current signal I_{mx} . We call these fluctuations back-action current noise. In the particular case of vanishing DC bias voltage (V_0) the expression of the back-action noise reads [52]:

$$S_I^{\text{ba}} = 8\lambda^2 S_x(\omega_2). \quad (7.19)$$

The factor 8 is due to the definition of the current noise and to the averages entering the mixing current detection. Once inserted into the definition of S^{add} it will simply give the intrinsic fluctuation of the oscillator generated by the electrons. In order to evaluate it we need to obtain $S_x(\omega_2)$, where typically ω_2 is very close to ω_0 .

7.3 Weak coupling regime

Let's begin to evaluate the behaviour of the device in the extreme weak coupling regime to be defined more precisely by Eq. (7.56) in the following. The spectrum S_x can

be obtained by solving the Langevin equation (7.12) by Fourier transform:

$$S_x(\omega) = \langle x(\omega)x(-\omega) \rangle = \frac{F_0^2 S_n(\omega)}{m^2 |\omega_m^2 - \omega^2 - i\gamma(x_e)\omega|^2}. \quad (7.20)$$

The charge noise is given by Eq. (7.14). In the limit $eV \ll k_B T$ one has $\sum_{\alpha,\beta} f_\alpha(1-f_\beta) \approx k_B T \delta(\omega - \mu)$ giving

$$S_n(\omega = 0) = \frac{2k_B T}{\pi \Gamma^2} \tau^2(z_e). \quad (7.21)$$

Assuming the worst case where $|\omega_2 - \omega_0| \ll \omega_0/Q$, with $Q = \omega_0/\gamma$ we have

$$S_x(\omega_2) = \frac{Q^2 F_0^2 S_n}{k^2}. \quad (7.22)$$

A convenient way of rewriting it is:

$$k S_x(\omega_2) = \frac{2Q^2}{\pi} \frac{\epsilon_P k_B T}{\Gamma^2} \quad (7.23)$$

where we introduced the coupling constant energy scale $\epsilon_P = F_0^2/k$. The quality factor induced by the electro-mechanical coupling can be obtained from Eq. (7.15):

$$Q = \frac{\pi \Gamma^2}{\epsilon_P \omega_0 \tau^2(z_e)}, \quad (7.24)$$

that gives

$$k S_x(\omega_0) = \frac{2\pi k_B T}{\epsilon_P} \frac{\Gamma^2}{\omega_0^2 \tau^2(z_e)} \quad (7.25)$$

We calculate the response function from Eq. (7.10):

$$\lambda = \frac{e^2 N V_1}{4\pi L} \frac{E_C}{\Gamma} \tau'(z_e) \approx F_0 \left(\frac{eV_1}{\Gamma} \right) \frac{e\tau'(z_e)}{4\pi}, \quad (7.26)$$

where $\tau' = d\tau/dz$, $L = C_g/C'_g$, N the number of electrons on the dot $\approx C_g V_g/e$, $E_C = e^2/2C_\Sigma$ the Coulomb energy of the island (see also 7.1).

Substituting the expressions for the shot noise Eq. (7.18) and the back-action noise Eq. (7.19) into Eq. (4.19) we obtain:

$$kS_x^{\text{add}} = \frac{k_B T}{\Gamma} \left[\alpha^{\text{ba}} Q^2 \frac{\epsilon_P}{\Gamma} + \alpha^{\text{shot}} \left(\frac{\Gamma}{eV_1} \right)^2 \frac{\Gamma}{\epsilon_P} \right] \quad (7.27)$$

with the numerical factors $\alpha^{\text{ba}} = 4\tau^2(z)/\pi$ and $\alpha^{\text{shot}} = 32\pi\tau(z)/(\tau'(z))^2$. One can in principle minimize this expression as a function of z and ϵ_P in order to find the best operational point. (Note that changing ϵ_0 allows to modify z_e , even if in a non linear way, since x_e depends also on ϵ_0 , as we will see in more details later.) In practice one prefers first to maximize the response function λ in order to have a strong signal, and then look to the optimal value of the coupling constant that minimizes the noise. The response function λ is maximized for $z_e = 1/\sqrt{3}$ where $\tau = 3/4$ and $\tau' = -3\sqrt{3}/8 \approx -0.65$. This gives $\alpha^{\text{ba}} \approx 0.716$, $\alpha^{\text{shot}} \approx 178.42$. Minimizing now with respect to ϵ_P we find

$$\epsilon_P^{\text{opt}} = \left(\frac{\alpha^{\text{shot}}}{\alpha^{\text{ba}}} \right)^{1/2} \frac{\Gamma^2}{QeV_1}, \quad (7.28)$$

with a minimum noise of

$$kS_x^{\text{opt}} = 2 \frac{k_B T}{\Gamma} (\alpha^{\text{ba}} \alpha^{\text{shot}})^{1/2} Q \frac{\Gamma}{eV_1}. \quad (7.29)$$

Since all the previous calculation are performed in the limit $eV_1 \ll k_B T \ll \Gamma$, the minimum value of the ratio Γ/eV_1 is 10. This gives for the optimal value of the coupling

$$\frac{\epsilon_P^{\text{opt}}}{\Gamma} \approx \frac{157.8}{Q}. \quad (7.30)$$

and the minimum of the added noise

$$kS_x^{\text{opt}} = 226.1 \frac{Qk_B T}{\Gamma}. \quad (7.31)$$

These expressions holds when the quality factors are controlled by the coupling of the oscillator to external degrees of freedom, like the surface phonons generated at the clamping points, or defects in the structures. In the special case of the damping dominated by the detection system Q is given by Eq. (7.24) (we neglect the ϵ_0 dependence of Q) and quite

surprisingly one finds that both the shot and the back-action noise decreases as $1/\epsilon_P$:

$$kS_x^{\text{add}} = \frac{k_B T}{\epsilon_P} \left[\frac{4\pi}{\tau^2} \left(\frac{\Gamma}{\omega_0} \right) + \frac{32\pi\tau}{\tau'^2} \right]. \quad (7.32)$$

In practice we have to limit the value of ϵ_P to the region where the weak-coupling approximation applies. We will see in the next section that the precise condition for that is given by Eq. (7.56). For typical values of the other parameters that we will use in the following for the numerical calculations ($\omega_0/\Gamma = 10^{-3}$, $eV_1/\Gamma = 0.1$, and $k_B T/\Gamma = 10^{-2}$) one finds a high value of the added noise of the order of $kS_x^{\text{add}} \approx 10^7$. Increasing the coupling reduces this value, but forces us to consider the effect of non-linearities.

7.4 Non-linear regime

When the coupling or the temperature increases the oscillation amplitude induced by the coupling to the electrons increases. One cannot neglect anymore the non-linear part of the effective force generated by the electrons on the oscillator. By evaluating explicitly $\langle n_d \rangle$ for $k_B T \ll \Gamma$ and for $eV = 0$ one obtains:

$$F(x) = -kx + F_0 \left[\frac{1}{2} + \frac{1}{\pi} \arctan \frac{\mu_0 - \epsilon_0 + F_0 x}{\Gamma} \right]. \quad (7.33)$$

The electronic force modifies significantly the equilibrium position of the oscillator that is no more in $x = 0$. Once we know the equilibrium position we can calculate the renormalized spring constant:

$$k' = - \left. \frac{dF}{dx} \right|_{x_e} = k - \frac{F_0^2}{\pi\Gamma} \tau(z_e) \quad (7.34)$$

It is convenient now to define new variables:

$$\tilde{\epsilon}_0 = \frac{\epsilon_0 - \mu_0 - \epsilon_P}{\Gamma}, \quad \text{and} \quad \tilde{x} = kx/F_0 - 1/2. \quad (7.35)$$

We now write the equilibrium equation for the oscillator, that is $F(x_e) = 0$. In terms of the newly introduced variables we have:

$$-\tilde{x}_e + \frac{1}{\pi} \arctan(\tilde{\epsilon}_0 - \pi\tilde{x}_e\tilde{\epsilon}_P) = 0 \quad (7.36)$$

where we have introduced also $\tilde{\epsilon}_P = \epsilon_P/(\pi\Gamma)$. It is convenient to use again the variable $z = \tilde{\epsilon}_0 - \pi\tilde{x}_e\tilde{\epsilon}_P$ and write the equilibrium equation as

$$\tilde{\epsilon}_0 = z_e - \tilde{\epsilon}_P \arctan z_e. \quad (7.37)$$

Written in this form it can be seen as the solution of the equilibrium equation in terms of z_e . The function is plotted in Fig. 7.1. One clearly sees that for $\tilde{\epsilon}_P > 1$ there are three

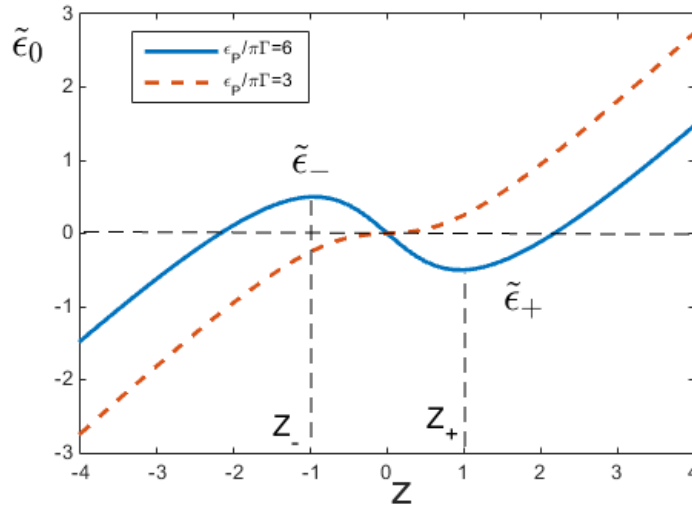


FIGURE 7.1: $\tilde{\epsilon}_0$ as function of z with the coupling $\epsilon_P/\pi\Gamma = 3, 6$. The appearance of the two extrema signals the appearance of the bistability

solutions, two stable and one unstable. We can find the condition for the appearance of the bistability by looking for the appearance of a maximum for the function $\tilde{\epsilon}_0(z)$. This gives $d\tilde{\epsilon}_0/dz = 0$ that has two solutions

$$z_{\pm} = \pm\sqrt{\tilde{\epsilon}_P - 1} \quad (7.38)$$

for $\tilde{\epsilon}_P > 1$. From these values we can find the two functions

$$\tilde{\epsilon}_{\pm} = z_{\pm} - \tilde{\epsilon}_P \arctan(z_{\pm}) = \pm[z_{\pm} - \tilde{\epsilon}_P \arctan(z_{\pm})]. \quad (7.39)$$

The system has only a single stable solution for $|\tilde{\epsilon}_0| > \tilde{\epsilon}_+$, and is instead bistable otherwise (see Fig. 7.2).

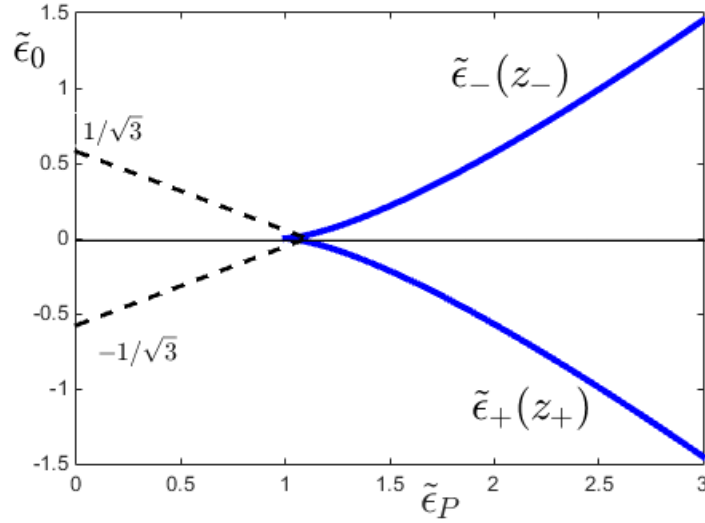


FIGURE 7.2: Stability diagram as a function of $\tilde{\epsilon}_0$ and $\tilde{\epsilon}_P$. The region between ϵ_+ and ϵ_- is bistable. The dashed lines give the values of $\tilde{\epsilon}_0$ for which $z = 1/\sqrt{3}$ (cf. Eq. (7.37)) and thus τ' is maximum.

The change of the stable points has an important consequence on the resonating frequency of the oscillator, that is renormalized (cf. Eq. (7.34)):

$$\omega_m^2/\omega_0^2 = 1 - \tilde{\epsilon}_P \tau^2(z_e), \quad (7.40)$$

where z takes the equilibrium value. For $\tilde{\epsilon}_0 = 0$ if $\tilde{\epsilon}_P < 1$ the only stable solution is for $z = 0$, while for $\tilde{\epsilon}_P > 1$ the solution in $z = 0$ is no more stable, and two new minima appears for $z \neq 0$. The behavior of the system in this case has been discussed in details in Ref. [26] where also analytical expressions for S_x have been derived. But when the stable solution is at $z = 0$ then $\tau'(z = 0) = 0$, and thus $\lambda = 0$. For the purpose of using the device as a displacement detection we need to work at $\tilde{\epsilon}_0 \neq 0$.

7.4.1 Weakly non-linear regime

Here we follow Ref. [26] to derive the analytical form of $S_x(\omega)$ for $\tilde{\epsilon}_0 \neq 0$ (and thus $z_e \neq 0$) when the quadratic part of the oscillator remains dominant. We begin by expanding the

potential around the equilibrium position x_e :

$$U(x) = U(x_e) - \sum_{n=2,4} \frac{1}{n!} \frac{\partial^{(n-1)} F}{\partial x^{(n-1)}} \Big|_{x_e} (x - x_e)^n + \dots \quad (7.41)$$

This gives for $\Delta U = U(x) - U(x_e)$ in terms of the $y = (x - x_e)F_0/\Gamma$

$$\Delta U(y)/\Gamma = ay^2 + by^3 + cy^4 \quad (7.42)$$

with

$$a = (1 - \tau\tilde{\epsilon}_P)/(2\pi\tilde{\epsilon}_P), \quad b = -\tau'/3!\pi, \quad c = -\tau''/4!\pi. \quad (7.43)$$

All these functions have to be evaluated at z equilibrium. In order to find the effect of the non-linearities on the spectrum a crucial quantity is the energy dependence of the resonating frequency

$$\frac{2\pi}{\omega_E} = 2m \int_{x_L}^{x_R} \frac{dx}{[2m(E - \Delta U(x))]^{1/2}}. \quad (7.44)$$

where $\Delta U(x_{L,R}) = E$ and $x_L < x_e < x_R$.

The resonating frequency is given by Eq. (7.44) that can be recast in the form

$$\frac{2\pi F_0}{(2m\Gamma)^{1/2}\omega_E} = I_1 + I_2, \quad (7.45)$$

with

$$I_1 = \int_{y_L}^0 dy (\tilde{E} - ay^2 - by^3 - cy^4)^{-1/2} \quad (7.46)$$

and I_2 the same integral taken between 0 and y_R . Here $y_{L,R} = (x_{L,R} - x_e)F_0/\Gamma$ and $\tilde{E} = E/\Gamma$. By definition $\tilde{E} = ay_{L,R}^2 + by_{L,R}^3 + cy_{L,R}^4$, we can thus substitute this expression in the integrals. We then introduce $\xi = y/y_{L,R}$. This gives:

$$I_{1,2} = \int_0^1 d\xi [a(1 - \xi^2) + by_{L,R}(1 - \xi^3) + cy_{L,R}^2(1 - \xi^4)]^{-1/2}. \quad (7.47)$$

This form is particularly convenient to perform the expansion for $y_{L,R} \ll 1$. In this limit the cubic and quartic terms can be treated as a perturbation of the quadratic term. At

order $y_{L,R}^2$ one has:

$$I_{1,2} = \int_0^1 d\xi \frac{1}{[a(1-\xi^2)]^{1/2}} \times \left[1 - \frac{by_{L,R}}{2a} \frac{(1-\xi^3)}{1-\xi^2} - \frac{cy_{L,R}^2}{2a} \frac{1-\xi^4}{1-\xi^2} + \frac{3b^2y_{L,R}^2}{8} \frac{(1-\xi^3)^2}{a^2(1-\xi^2)^2} \right]. \quad (7.48)$$

All the integrals can be performed giving:

$$I_{1,2} = \frac{\pi}{2a^{1/2}} \left[1 - \frac{2by_{L,R}}{\pi a} + y_{L,R}^2 \left(\left(\frac{3}{\pi} - \frac{45}{64} \right) \frac{b^2}{a^2} - \frac{3c}{4a} \right) \right] \quad (7.49)$$

Solving perturbatively the equation for $y_{L,R}$ we find at order $y_{L,R}^3 \sim \tilde{E}^{3/2}$:

$$y_{L,R} = \mp \left(\frac{\tilde{E}}{a} \right)^{1/2} \left[1 \pm \frac{b}{2a} \left(\frac{\tilde{E}}{a} \right)^{1/2} - \frac{c\tilde{E}}{2a} \right] \quad (7.50)$$

In particular in order to evaluate $I_1 + I_2$ we need the sum $y_L + y_R = -b\tilde{E}/a$. We finally obtain:

$$I_1 + I_2 = \frac{\pi}{a^{1/2}} - \frac{\tilde{E}}{4\pi^5 a^{5/2}} C \quad (7.51)$$

with

$$C(z, \tilde{\epsilon}_P) = \pi^4 \left[\frac{3}{2}c - \frac{b^2}{a} \left(\frac{47}{8} - \frac{2}{\pi} \right) \right]. \quad (7.52)$$

From this one can readily obtain the derivative of ω_E :

$$\omega'_E(0) \equiv \frac{d\omega_E}{dE}(0) = C \frac{\omega_m}{\Gamma} \frac{\tilde{\epsilon}_P^2}{(1 - \tau\tilde{\epsilon}_P)^2}. \quad (7.53)$$

One can then simply use the expansion

$$\omega_E = \omega_m + \omega'_E(0)E + \dots \quad (7.54)$$

and find that the spectrum has the same form found in Ref. [26] supplemental materials:

$$S_x(\omega) = \frac{\pi(\omega - \omega_m)}{m\omega_m\omega'_E{}^2 k_B T} e^{-(\omega - \omega_m)/\omega'_E(0)k_B T}. \quad (7.55)$$

One relevant difference is that ω'_E can be either positive or negative, the cubic term induces a reduction of the frequency, while the quartic one an increase. The spectrum Eq. (7.55) has a maximum for $\omega = \omega_m + \omega'_E k_B T$ and a full width at half height of $\Delta\omega = \Delta_2 |\omega'_E(0)| k_B T$, with $\Delta_2 \approx 2.446$.

With these expressions we can first compare with the purely dissipative calculation of the previous section and find for which value of the coupling constant the width induced by the dissipation (γ) is of the same order of the width induced by the non-linearities ($\Delta\omega$):

$$\tilde{\epsilon}_P \approx \frac{\omega_0}{k_B T} \frac{\tau^2}{\Delta_2 C} \ll 1 \quad (7.56)$$

where the last disequality comes from the classical hypothesis on the oscillator $\hbar\omega/k_B T \ll 1$. Changing the equilibrium position modifies the numerical factor C , but it has not a dramatic effect. This is also the condition of validity of the weak coupling approximations.

In order to obtain the sensibility of the device in the weakly non-linear regime we need the maximum of S_x (in the usual pessimistic assumption that ω_2 is closer to ω_1 than the width of the resonance):

$$kS_x^{\max} = \frac{\pi e^{-1}}{(1 - \tilde{\epsilon}_P \tau) \omega'_E}. \quad (7.57)$$

Note that the maximum of the spectrum does not depend on the temperature. This may seem surprising at a first glance, but actually it follows from the fact that the integral of the spectrum is dominated by the quadratic contribution that is proportional to the temperature (equipartition theorem), but now the width of the distribution also is proportional to T , thus the only way to keep the normalization is that the maximum does not depend on T .

We can now obtain the form of the added noise:

$$kS_x^{\text{add}} = 2kS_x^{\max} + 8\pi \frac{k_B T}{\epsilon_P} \frac{\tau}{\tau'^2} \left(\frac{\Gamma}{eV_1} \right)^2. \quad (7.58)$$

Explicitly:

$$kS_x^{\text{add}} = \frac{2\pi}{eC} \frac{\Gamma}{\omega_0} \frac{(1 - \tilde{\epsilon}_P \tau)^{1/2}}{\tilde{\epsilon}_P^2} + 8\pi^2 \frac{k_B T}{\Gamma} \frac{1}{\tilde{\epsilon}_P} \frac{\tau}{\tau'^2} \left(\frac{\Gamma}{eV_1} \right)^2. \quad (7.59)$$

We set $z = 1/\sqrt{3}$ that maximizes λ . We then find that both terms in Eq. (7.59) are monotonically decreasing as a function of $\tilde{\epsilon}_P$. That is normal for the second term, but unusual for the first one that encodes the back-action of the detection system. The minimum of the imprecision noise is thus obtained at the maximum value of $\tilde{\epsilon}_P$ for which the above expressions are still valid.

In order to find the validity region we evaluate the amplitude of fluctuation of the variable y . Neglecting the quartic and cubic terms one finds from the equipartition theorem $\langle y^2 \rangle = k_B T / 2a\Gamma$. The conditions on the smallness of the cubic and quartic terms read then $a \gg b\langle y^2 \rangle^{1/2}$ and $a \gg b\langle y^2 \rangle$. Explicitly for the cubic term:

$$\frac{k_B T}{\Gamma} \ll \frac{(3!)^2 (1 - \tau\tilde{\epsilon}_P)^3}{2\pi\tau'^2 \tilde{\epsilon}_P^3} \quad (7.60)$$

and for the quartic term

$$\frac{k_B T}{\Gamma} \ll \frac{1}{12\pi^3 |\tau''|} \frac{(1 - \tau\tilde{\epsilon}_P)^2}{\tilde{\epsilon}_P^2}. \quad (7.61)$$

If we choose as usual the value $z = 1/\sqrt{3}$ to maximize λ , we have that the quartic term of the expansion is exactly vanishing at that point, leaving only the cubic part. We see that the condition given by Eq. (7.60) can be always be satisfied since even for $\tilde{\epsilon}_P = 1$ it reads $k_B T / \Gamma \ll 4/3\pi \approx 0.42$. Note that this is not possible for the case $z = 0$, for which the cubic term vanishes and the quadratic condition becomes $k_B T / \Gamma \ll (1 - \tilde{\epsilon}_P)^2 / \tilde{\epsilon}_P^2 4! \pi^3$ that vanishes at $\tilde{\epsilon}_P = 1$. For this value there is a crossover to a purely quartic behaviour of the oscillator. For $z \neq 0$ the crossover between the quadratic and cubic correction happens for

$$1 = \frac{k_B T}{\Gamma} \frac{\tilde{\epsilon}_P}{1 - \tilde{\epsilon}_P} \frac{\tau''^2}{\tau'^2} \frac{\pi}{16}, \quad (7.62)$$

that defines a small region around the line $z = 0$ and $\tilde{\epsilon}_P < 1$.

Coming back to the expression for S_x^{add} we set $\tilde{\epsilon}_P = 1$ and $z = 1/\sqrt{3}$ to obtain the optimal value:

$$k S_x^{\text{opt}} = 3.4 \frac{\Gamma}{\omega_0} + 140 \left(\frac{\Gamma}{eV_1} \right)^2 \frac{k_B T}{\Gamma}. \quad (7.63)$$

We see that the last term is essentially the same that we calculated in the weak-coupling regime, where the dissipation determines the width. Here we simply could push the expression to its limit by calculating the first part that includes the non-linear contribution.

The first term is large, due to the small value of ω_0 and independent of the temperature (provided it is finite). The reason has been given above and the consequences are that for

$$\frac{k_B T}{\Gamma} < 0.024 (eV_1/\Gamma)^2 \approx 2.4 \cdot 10^{-4} \quad (7.64)$$

the current noise becomes negligible with respect to the intrinsic mechanical fluctuations. Using the same parameters of before ($\omega_0/\Gamma = 10^{-3}$, $eV_1/\Gamma = 0.1$, and $k_B T/\Gamma = 10^{-2}$) we find an optimal value of $kS_x^{\text{opt}} \approx 3400$, in good agreement with the numerical results of the next section.

7.5 Numerical evaluation of the fluctuations

In the previous section we have evaluated the added noise and the response function in different regimes performing some approximations on the evaluation of the stochastic fluctuations. For instance we evaluated the response function by setting z at the equilibrium value, but a definition that takes into account the fluctuations reads:

$$\lambda = \frac{F_0 e V_1}{4\pi\Gamma\hbar L} \int dx dp P_{st}(x, p) \tau'(z_x). \quad (7.65)$$

In order to find the stationary $P_{st}(x, p)$ that solves the Fokker-Planck equation we discretize the equation and solve numerically the associated linear problem. Defining the Fokker-Planck operator as \mathcal{L} such that

$$\partial_t P = \hat{\mathcal{L}}P \quad (7.66)$$

one can also find an explicit expression for the displacement spectrum [19]:

$$S_x(\omega) = -2\text{Tr}[\hat{x} \frac{\hat{\mathcal{L}}}{\omega^2 + \hat{\mathcal{L}}^2} \hat{x} P_{st}], \quad (7.67)$$

where all the terms with a hat in Eq. (7.67) are super-operators acting in the space of probability, P_{st} is a vector solution of $\hat{\mathcal{L}}P_{st} = 0$ and $\hat{x}(t) = \hat{x}(t) - \langle x \rangle$ (see Ref. [19] for more details). Using this approach we can calculate explicitly the average of λ .

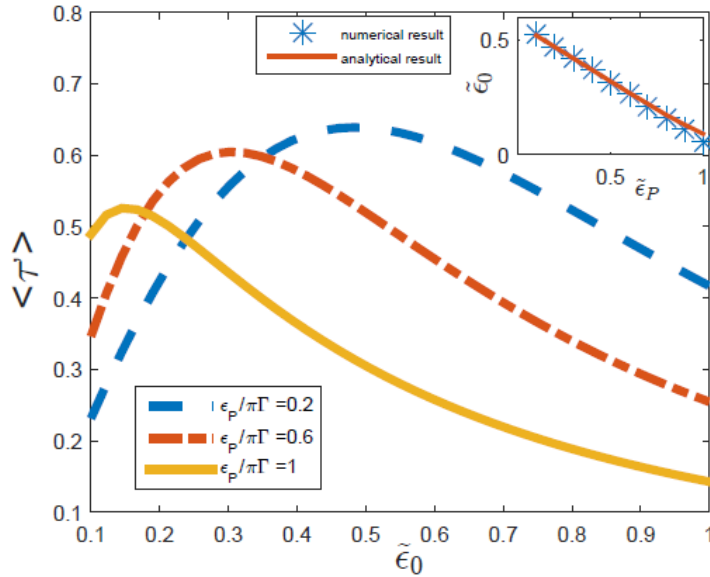


FIGURE 7.3: $\langle \tau' \rangle$ as function of $\tilde{\epsilon}_0$ for different values of the coupling constant $\tilde{\epsilon}_P = 0.2, 0.6, 1$. In this figure and in the following ones the other parameters are $\omega_0/\Gamma = 10^{-3}$, $eV_1/\Gamma = 0.1$ and $k_B T/\Gamma = 10^{-2}$.

In the following all the figures are plotted for the following values of the parameters: $\omega_0/\Gamma = 10^{-3}$, $eV_1/\Gamma = 0.1$ and $k_B T/\Gamma = 10^{-2}$. We show in Fig. 7.3 the average of τ' , that is the only part that depends on the fluctuations.

Also the low frequency ($\omega \ll \Gamma$) shot noise has to be averaged over the stationary distribution probability:

$$S_I^{\text{shot}} = \frac{2k_B T e^2}{\pi} \int dx dp P(x, p, t) \tau(x). \quad (7.68)$$

From these two expressions we can study the dependence of $S_I^{\text{shot}}/\lambda^2$ as a function of $\tilde{\epsilon}_0$ for different values of the coupling constant. We show the result in Fig. 7.4. One sees that for higher coupling one reaches higher sensitivity. The main origin of the $\tilde{\epsilon}_0$ dependence remains that given by the average of τ' , with a minimum that moves at lower values $\tilde{\epsilon}_0$ simply by the relation between z and $\tilde{\epsilon}_0$ for given ϵ_P [cf. Fig. 7.2 and Eq. (7.37)].

Finally performing the calculation of the spectrum we show in Fig. 7.5 the dependence of the maximum of the spectrum compared with the analytical approximations for the case $\tilde{\epsilon}_0 = 0$ and as a function of $\tilde{\epsilon}_P$.

This figure shows the nice agreement between the weakly non-linear approximation (Eq. (7.57)) with the numerics for till $\tilde{\epsilon}_P \approx 0.7$, as expected. At very weak value of the

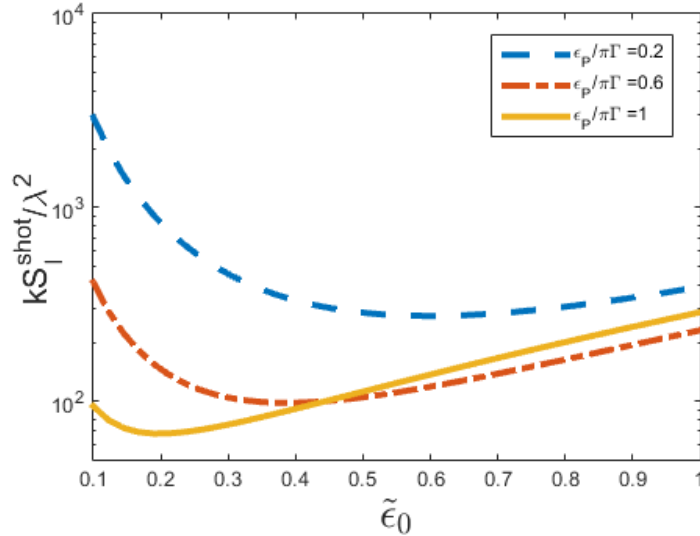


FIGURE 7.4: The $\langle \tau/\tau'^2 \rangle$ as a function of $\tilde{\epsilon}_0$ with the coupling $\epsilon_P = 0.2, 0.6, 1$.

coupling constant $\tilde{\epsilon}_P = 0.1$ we believe that our numerical calculation is not sufficiently accurate to correctly reproduce the value of the maximum of the spectrum, since the peak is very narrow. The weak coupling (dissipation dominated) analytical result Eq. (7.25) is shown dashed. Unfortunately we cannot access with the accuracy of the numerical calculation to the region where the dissipation controls the width, due to the fact that the response function is very sharp. The value of ϵ_P for which the dashed and the full line crosses is the crossover value when the non-linearities take over.

We can now come to the numerical evaluation of the added noise Eq. (4.19) for two different values of the coupling constant: $\tilde{\epsilon}_P = 0.8$ and 1. The result is shown in Fig. 7.6 as a function of $\tilde{\epsilon}_0$. If we compare these results with those shown in Fig. 7.3, for instance for $\tilde{\epsilon}_P = 1$, we see that the position of the minimum moved at slightly lower values of $\tilde{\epsilon}_0$, but in particular the absolute value of the fluctuation increased of more than a decade. This is due to the contribution of the fluctuations induced by the thermal motion in the non-linear regime.

We can conclude that the best sensibility of the device is found for the largest coupling available before the bistability: $\tilde{\epsilon}_P = 1$.

One could in principle explore also the bistable region, but the presence of two minima that are quasi degenerate for $\tilde{\epsilon}_0 \ll 1$ introduce an additional source of low-frequency noise. As discussed in Ref. [26] a strong peak at low frequency appears at the transition

and is due to hopping of the system between the two stable points. The noise persists for a large region after $\tilde{\epsilon}_P = 1$ increasing of 6 orders of magnitude between $\tilde{\epsilon}_P = 1$ and $\tilde{\epsilon}_P = 1.2$. A second limitation of the bistable region is the strong reduction of the current. The two stable points for large value of the coupling corresponds to the empty and full dot. This is particularly clear for $\epsilon_0 = 0$. From Eq. (7.37) and $\tilde{\epsilon} \gg 1$ one finds

$$z_e \approx \pm \frac{\pi}{2} \tilde{\epsilon}_P. \quad (7.69)$$

leading to a transparency of the junction of the order of $\tau \sim (\pi \tilde{\epsilon}_P / 2)^{-2} \ll 1$. The current through the device is thus very weak.

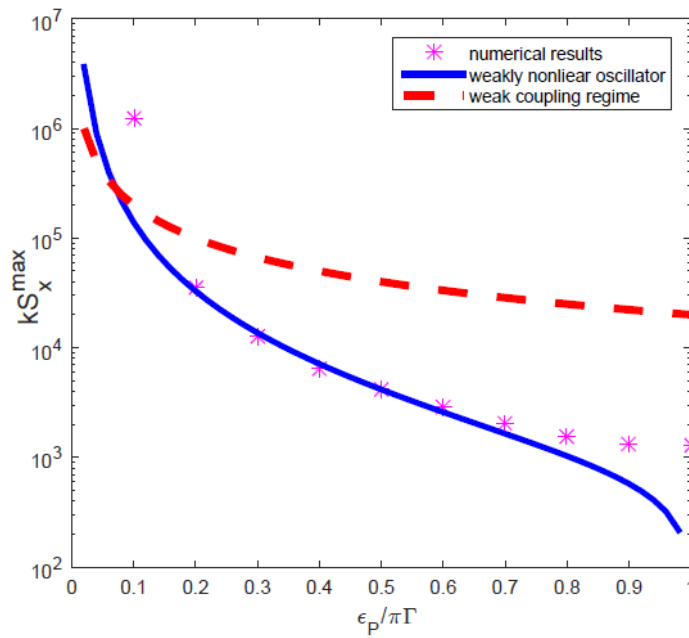


FIGURE 7.5: The maximum of the displacement spectrum (stars), S_{xx}^{\max} as function of ϵ_P compared to the two analytical expressions valid in the weak coupling regime (dashed) and in the weakly non-linear regime (full line).

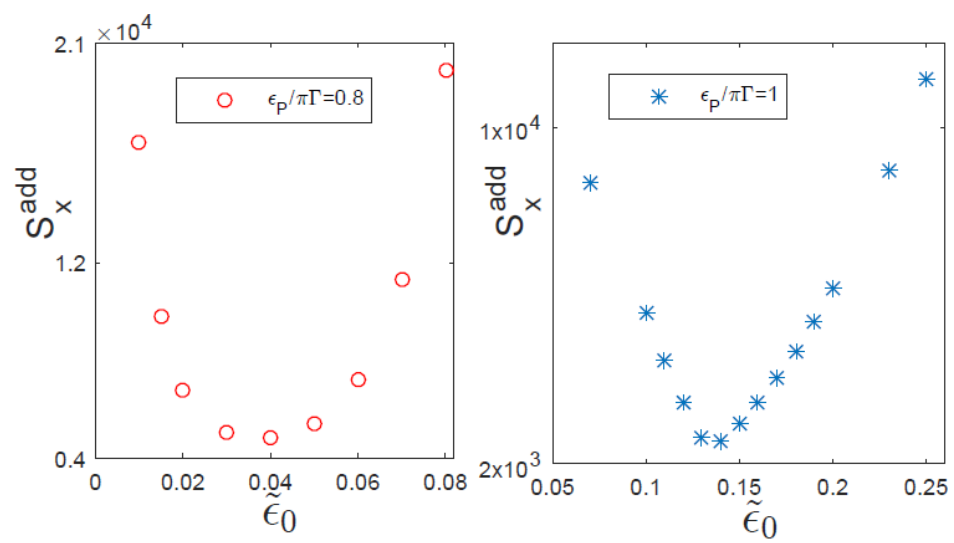


FIGURE 7.6: The added noise as a function of $\tilde{\epsilon}_0$ for $\epsilon_P = 0.8$ (left) and $\epsilon_P = 1$ (right). The other parameters are the same of the previous figures

Chapter 8

Conclusions

In this thesis we have studied theoretically the sensitivity of the mixing-current technique. We first found general expressions valid when the oscillator resonating frequency is comparable or larger of the transfer rate of electrons. We find that a reduction of the amplification factor of the order of $(\Gamma_0/\omega_D)^2$ is expected. This effect should be relatively small in most practical experimental realizations. We then analysed the fundamental limitations due to the intrinsic noise present in the (current) signal and the effect of the back-action fluctuations.

For the incoherent tunnelling regime ($\Gamma \ll k_B T$), on general grounds one finds that an optimal value of the electromechanical coupling (ϵ_P) exists that minimizes the added noise. This value is larger than what is realized in the present experiments, showing that increasing the coupling allows to reach higher sensitivity. At finite temperature the relevant parameter is the ratio $\epsilon_P/k_B T$ and values of the order of 1 are needed to reach the optimal minimum added noise. At $eV \gg k_B T$ the relevant parameter is instead ϵ_P/eV . In all cases the scale of the sensitivity is given by $E_C/\Gamma_0 k$. We find that single-electronic level SET allows for a better resolution than the metallic SET by a parametric factor $E_C/k_B T$. Optical means can detect CNTs displacement with good accuracy, even if the small size of the object does not allows to reach the spectacular sensitivity obtained with macroscopic mirrors. A sensitivity of $5 \cdot 10^{-22} \text{ m}^2/\text{Hz}$ as been reported [53] by cavity-enhanced optical detection of CNTs.

We considered only classical fluctuations. It seems difficult to use the mixing technique to reach the quantum limit of detection, since the effective temperature of the oscillator, even at vanishing temperature, is of the order of eV that typically needs to be larger than $\hbar\omega_m$. On the other side it may be instructive to compare the sensitivity found at vanishing temperature with the zero point fluctuations spectrum at resonance: $S_x^{\text{SQL}} = 2\hbar\omega_m/k\gamma$. One sees that the ratio to the typical mixing-current technique added noise at zero temperature is $10^{-2}(\hbar\omega_m/E_C)(\Gamma/\gamma)(\epsilon_P/E_C)$, since $\Gamma/\gamma \gg 1$, for sufficiently large ϵ_P the added noise can be of the same order of the zero-point fluctuations.

We conclude that the sensitivity of the mixing technique can still be improved by increasing the electromechanical coupling till reaching ϵ_P of the order of the temperature or the Coulomb blockade energy where the back-action will be of the same order of the intrinsic current noise of the device.

For the coherent tunnelling regime ($\Gamma \gg k_B T$), we have investigated theoretically the sensitivity of the mixing current technique when the oscillator is measured by coupling it to a quantum dot. In order to obtain the best sensitivities one finds that increasing the coupling is always helpful, mainly for the increase in the value of the response function λ , and thus due to a the reduction of the intrinsic electronic current noise once referred back to the displacement. In principle the best coupling value is determined by a compromise between the back-action noise and the electronic noise, but in our case we have shown that the system undergoes a bistability before reaching this ideal value. We thus considered in details the behaviour of the device close to the bistability region and found the best sensitivity that can be achieved with the device, before entering the bistable regions. We found that the in weak coupling regime the displacement fluctuation has a standard lorentian form with a width controlled by the electronically induced dissipation. In this limit the best sensitivity that can be obtained is given by Eq. (7.32). Its validity is constrained by the condition Eq. (7.56) on the coupling constant, thus limiting its scope to a very weak-coupling regime and relatively low value of sensitivity. For larger coupling constant we were able to obtain analytically the form of the displacement spectrum and thus to obtain the sensitivity of the device along the line in the $\tilde{\epsilon}_0 - \epsilon - P$ plane defined by $z = 1/\sqrt{3}$ where λ is maximal. The analytical approach is based on a weak-non linear expansion, that on the line $z = 1/\sqrt{3}$ holds all the way till the critical value $\tilde{\epsilon}_P = 1$. The

best sensitivity is given by Eq. (7.59) or for $\tilde{\epsilon}_P = 1$ by Eq. (7.63). We then performed numerical calculation of λ and of the S_x^{add} that allowed to confirm the findings of the previously described analytical results and to observe the small deviations. We did not investigate in details the bistable region, since the telegraph noise and the reduction of the current appears to deteriorate seriously the quality of the detectors.

In conclusions this study indicates clearly that even in presence of the non-linear fluctuations close to the bistability one finds that increasing the coupling always improve the sensitivity of the device for the detection of the amplitude of oscillation. It is interesting to investigate this coherent case in the bistable region and find how higher sensitivity can be pushed in the strong coupling limit by this mixing technique.

Appendix A

Full Counting Statistics for periodically modulated system

In this Appendix we derive expressions for the full counting statistics of transport for a system described by a Master equation and driven by two harmonic signals. We develop a formal theory that allows in principle to obtain all the time-dependent cumulants of the number of charges in one of the leads, and thus of the current passed through the device. This method was developed to obtain the fluctuations of the mixing current technique Ref. [52] with a higher order accuracy than that was used in the Chapter 4. In the end we realized that this level of accuracy was not needed for the purpose of obtaining the sensitivity of the mixing-current technique, but the method developed is interesting by itself and can be applied to any incoherent transport device in presence of two driving sources. For these reasons we report in this appendix these results, that are part of the work of the thesis but are not necessary for the results presented in the main part of the manuscript.

A.1 Model and the rate equation

In the section we introduce the charge-transfer probability distribution with the general model , and derive a formal expression for the probability distribution of the

number of transferred particles from one lead, taken as a reference.

Let us consider the probability $P_n(N, t)$ that N charges are in the left lead of a SET, while the central island is in the state n . We define its Fourier transform:

$$P_n(\chi) = \sum_N e^{i\chi N} P_n(N, t). \quad (\text{A.1})$$

We assume that we have an equation for this quantity that can be written as follows:

$$\dot{P}_n(\chi, t) = \sum_m M_{nm}(\chi, t) P_m(\chi, t), \quad (\text{A.2})$$

With the initial condition $P_n(\chi, 0)$. In the following we will write the same equation in vector form:

$$\dot{P}(\chi, t) = M(\chi, t) P(\chi, t) \quad (\text{A.3})$$

here P is a vector.

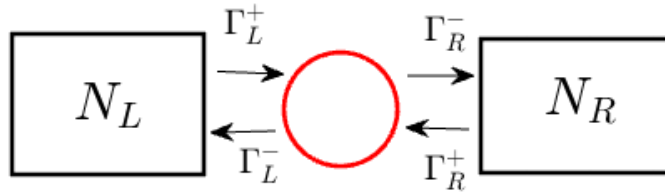


FIGURE A.1: The charge transfers in the SET, $\Gamma_{L,(R)}^\pm$ corresponding to four tunnelling process

This equation can be derived from the master equation for the charge transfer. Specifically in the case considered in the thesis if we define $P_{N_L, n}$ the probability of that two states $n = 0, 1$ (see Chapter 5) of the dot with that of left side is N_L the equation reads (Fig.A.1):

$$\dot{P}_{N_L, 0} = -\Gamma^+ P_{N_L, 0} + \Gamma_L^- P_{N_L-1, 1} + \Gamma_R^- P_{N_L, 1} \quad (\text{A.4})$$

$$\dot{P}_{N_L, 1} = -\Gamma_- P_{N_L, 1} + \Gamma_L^+ P_{N_L+1, 0} + \Gamma_R^+ P_{N_L, 0} \quad (\text{A.5})$$

here We define $\Gamma_R^{+(-)}$ as the rate for adding (subtracting) one electron on (from) the central island through the left tunnel junction. Similarly we define $\Gamma_R^{+(-)}$ for the right

junction, $\Gamma^\alpha = \Gamma_L^\alpha + \Gamma_R^\alpha$, with $\alpha = \pm$, $\Gamma_L = \Gamma_L^+ + \Gamma_L^-$, $\Gamma_R = \Gamma_R^+ + \Gamma_R^-$, and $\Gamma^T = \Gamma^+ + \Gamma^-$, see Chapter.5.

take the Fourier transform of the master equation,

$$P_{\chi,n} = \sum_N e^{-i\chi N} P_{N,n} \quad (\text{A.6})$$

we obtain the matrix form of the master equation:

$$\dot{P}_{\chi,0} = M(\chi)P_\chi \quad (\text{A.7})$$

with

$$M(\chi) = \begin{bmatrix} -\Gamma^+ & \Gamma_L^- e^{i\chi} + \Gamma_R^- \\ \Gamma_L^+ e^{-i\chi} + \Gamma_R^+ & -\Gamma^- \end{bmatrix}$$

then we can write the solution in the following form:

$$P(\chi, t) = e^{Mt} P(\chi, 0) \quad (\text{A.8})$$

Let's now assume that the time dependence of $M(\chi, t)$ is due to two cosine terms:

$$M(\chi, t) = M(\chi, \epsilon_1 \cos \omega_1 t, \epsilon_2 \cos \omega_2 t) \quad (\text{A.9})$$

we assume that ϵ_i are two small dimensionless parameters and we expand the expression of M .

$$M(\chi, t) = \sum_{n,m} M_{nm}(\chi) \epsilon_1^n \epsilon_2^m \cos^n \omega_1 t \cos^m \omega_2 t \quad (\text{A.10})$$

We want now write M as a sum of harmonics:

$$M(\chi, t) = \sum_{pq=-\infty}^{+\infty} N_{pq}(\chi) e^{ip\omega_1 t + iq\omega_2 t} \quad (\text{A.11})$$

Expanding the expression [A.10](#) we have:

$$M = \sum_{n,m} M_{nm}(\chi) \frac{\epsilon_1^n \epsilon_2^m}{2^{m+n}} (e^{i\omega_1 t} + e^{-i\omega_1 t})^n (e^{i\omega_2 t} + e^{-i\omega_2 t})^m \quad (\text{A.12})$$

That can be further be written as:

$$M = \sum_{n,m=0}^{\infty} M_{nm}(\chi) \frac{\epsilon_1^n \epsilon_2^m}{2^{m+n}} \sum_{k=0}^n \sum_{l=0}^m \binom{n}{k} \binom{m}{l} e^{i(n-2k)\omega_1 t + i(m-2l)\omega_2 t} \quad (\text{A.13})$$

We can reorder this sum. One should notice that the k and l terms can be reordered independently, and that for each value of n and m there is only one harmonics of order p appearing for $p = n - 2k$ (remember that $0 \leq k \leq n$). This gives:

$$N_{pq}(\chi) = \sum_{m_1, m_2=0}^{\infty} \frac{\epsilon_1^{|p|+2m_1}}{2^{|p|+2m_1}} \binom{|p|+2m_1}{(|p|-p)/2+m_1} \frac{\epsilon_2^{|q|+2m_2}}{2^{|q|+2m_2}} \binom{|q|+2m_2}{(|q|-q)/2+m_2} M_{|p|+2m_1, |q|+2m_2} \quad (\text{A.14})$$

Note that the order in ϵ increases with $|p|$ and $|q|$.

A.2 Solution of the equation

Let's now use the form [A.11](#) to solve the equation of motion. We begin by introducing the Laplace transform:

$$\tilde{P}(\chi, z) = \int_0^{\infty} dt e^{-zt} P(\chi, t) \quad (\text{A.15})$$

with $\text{Re}(z) > 0$. With this definition of the Laplace transform we have

$$\int_0^{\infty} dt e^{-zt} \dot{P}(\chi, t) = - \int_0^{\infty} dt (-z) e^{-zt} P(\chi, t) + e^{-zt} P(\chi, t) \Big|_0^{\infty} \quad (\text{A.16})$$

that finally gives:

$$\int_0^{\infty} dt e^{-zt} \dot{P}(\chi, t) = z \tilde{P}(\chi, z) - P(\chi, 0) \quad (\text{A.17})$$

The equation of motion becomes thus:

$$z \tilde{P}(\chi, z) - P(\chi, 0) = \sum_{pq} N_{pq}(\chi) \int_0^{\infty} dt e^{-zt + i(p\omega_1 + q\omega_2)t} P(\chi, t) \quad (\text{A.18})$$

We introduce the inverse of the Laplace transform:

$$P(t) = \int \frac{dz}{2\pi i} e^{zt} \tilde{P}(z) \quad (\text{A.19})$$

the integral has to be performed on a path going from $-i\infty$ to $+i\infty$ and remaining in the the positive real semispace ($\text{Re}z > 0$). This gives:

$$z\tilde{P}(\chi, z) = P(\chi, 0) - \sum_{pq} N_{pq}(\chi) \int \frac{dz'}{2\pi i} \frac{\tilde{P}(z')}{-z + z' + i(p\omega_1 + q\omega_2)} \quad (\text{A.20})$$

where we have used that $\text{Re}(z - z') > 0$. Here there is subtle point. We integrate in the complex plane in a line $z' = \eta + is$, with s going from $-\infty$ to $+\infty$, and $\eta > 0$ and infinitesimal. In particular we choose $\eta < \text{Re}\lambda_n$, where λ_n are the eigenvalues of N_{00} , this will be clear later, since we will find that the poles of $\tilde{P}(z)$ are of the form $\lambda_n + i\omega$. Thus using this line we leave all the poles of $\tilde{P}(z')$ on the right, we can then deform the contour to bring it to the left. We will need to avoid the poles in the denominator, that are all on the imaginary axis. Each pole will contribute with its residue. We thus find:

$$z\tilde{P}(\chi, z) = P(\chi, 0) + \sum_{pq} N_{pq}(\chi) \tilde{P}(\chi, z - ip\omega_1 - iq\omega_2) \quad (\text{A.21})$$

That is the final form of the equation of motion.

We proceed now to its solution as an expansion in ϵ . At zeroth order we find

$$[z - N_{00}(\chi)]\tilde{P}(\chi, z) = P(\chi, 0) \quad (\text{A.22})$$

Let's now introduce the left v_n and right w_n eigenvectors of $N_{00}(\chi)$ for the eigenvalue $\lambda_0(\chi)$. The solution of the equation reads:

$$\tilde{P}(\chi, z) = [z - N_{00}(\chi)]^{-1} P(\chi, 0) = \sum_n v_n \frac{(w_n, P(\chi, 0))}{z - \lambda_n} \quad (\text{A.23})$$

where (w, v) is the scalar product, and we assumed a normalization of the states such that $(w_n, v_n) = \delta_{nm}$. This gives immediately the time dependent solution:

$$\tilde{P}(\chi, t) = \sum_n v_n(w_n, P(\chi, 0)) e^{\lambda_n t} \quad (\text{A.24})$$

as it can be also found directly without the Laplace transform. We will assume that the eigenvectors are ordered by real part, so that λ_0 is the one with the smallest real part, and it is the one that vanishes for $\chi \rightarrow 0$. We can calculate the average number of particles and its fluctuation as follows:

$$\langle N \rangle = \frac{\partial P(\chi, t)}{\partial i\chi} \quad \langle N^2 \rangle = \frac{\partial^2 P(\chi, t)}{\partial (i\chi)^2} \quad (\text{A.25})$$

The current is simply $d\langle N \rangle/dt$, it will in general contain a constant and many oscillating terms.

Let's now solve the problem perturbatively at first order in N_{pq} with $(p, q) \neq (0, 0)$. It is sufficient to substitute the zeroth order solution back into the equation for P and neglect higher order in N . To do this first write [A.21](#) separating the part that vanishes for small driving:

$$P(\chi, z) = (z - N_{00})^{-1} P(\chi, 0) + \sum_{pq \neq 0} (z - N_{00})^{-1} N_{pq}(\chi) P(z - ip\omega_1 - iq\omega_2) \quad (\text{A.26})$$

We substitute now the zeroth order solution [A.23](#) into this equation:

$$P(\chi, z) = (z - N_{00})^{-1} P(\chi, 0) + \sum_{pq \neq 0} (z - N_{00})^{-1} N_{pq} (z - ip\omega_1 - iq\omega_2 - N_{00})^{-1} P(\chi, 0) \quad (\text{A.27})$$

This equation can be easily Laplace transformed by projecting on the base of eigenvectors of N_{00} . We have:

$$P^{(1)}(\chi, t) = \sum_{nm} \sum_{p, q \neq 0} v_m(w_m, N_{pq} v_n)(w_n, P(0)) \frac{[e^{\lambda_n t + i\omega_1 p t + i\omega_2 q t} - e^{\lambda_m t}]}{\lambda_n - \lambda_m + i\omega_1 p + i\omega_2 q} \quad (\text{A.28})$$

to be added to [A.21](#). For long time scales we can discard the contributions of all eigenvectors but the lowest one. This gives for the full $P(t)$:

$$P(\chi, t) = v_0(\chi)(w_0, P(0))e^{\lambda_0 t} \left(1 - \sum_{q,p \neq 0} \frac{(w_0, N_{qp} v_0)}{i\omega_1 p + i\omega_2 q} \sum_{q,p \neq 0} \frac{(w_0, N_{qp} v_0)}{i\omega_1 p + i\omega_2 q} e^{i\omega_1 p t + i\omega_2 q t} \right) \quad (\text{A.29})$$

From this expression we can readily calculate the time evolution of the averages of N^n . It is sufficient to perform the derivative with respect to $i\chi$ and then to project the results over w_0 for $\chi = 0$.

References

- [1] K. L. Ekinici, X. M. H. Huang, and M. L. Roukes. Ultrasensitive nanoelectromechanical mass detection. *Appl. Phys. Lett.*, 84:4469, 2002.
- [2] B. Lassagne, D. Garcia-Sanchez, A. Aguasca, and A. Bachtold. Ultrasensitive Mass Sensing with a Nanotube Electromechanical Resonator. *Nano Lett.*, 8(11):3735–3738, November 2008.
- [3] J. Chaste, A. Eichler, J. Moser, G. Ceballos, R. Rurali, and A. Bachtold. A nanomechanical mass sensor with yoctogram resolution. *Nature Nanotechnology*, 7(5):301–304, April 2012.
- [4] H. J. Mamin, M. Poggio, C. L. Degen, and D. Rugar. Nuclear magnetic resonance imaging with 90-nm resolution. *Nat Nano*, 2(5):301–306, 2007.
- [5] M. Poggio, M. P. Jura, C. L. Degen, M. A. Topinka, H. J. Mamin, D. Goldhaber-Gordon, and D. Rugar. An off-board quantum point contact as a sensitive detector of cantilever motion. *Nat Phys*, 4(8):635–638, 2008.
- [6] P. Rabl, P. Cappellaro, M. V. Gurudev Dutt, L. Jiang, J. R. Maze, and M. D. Lukin. Strong magnetic coupling between an electronic spin qubit and a mechanical resonator. *Phys. Rev. B*, 79(4):041302, January 2009.
- [7] Olivier Arcizet, Vincent Jacques, Alessandro Siria, Philippe Poncharal, Pascal Vincent, and Signe Seidelin. A single nitrogen-vacancy defect coupled to a nanomechanical oscillator. *Nature Physics*, 7(11):879–883, 2011.
- [8] Vadim Puller, Brahim Lounis, and Fabio Pistolesi. Single Molecule Detection of Nanomechanical Motion. *Phys. Rev. Lett.*, 110(12):125501, March 2013.

-
- [9] J. Moser, A. Eichler, J. Güttinger, M. I. Dykman, and A. Bachtold. Nanotube mechanical resonators with quality factors of up to 5 million. *Nat Nano*, 9(12):1007–1011, 2014.
- [10] J. Moser, J. Güttinger, A. Eichler, M. J. Esplandiu, D. E. Liu, M. I. Dykman, and A. Bachtold. Ultrasensitive force detection with a nanotube mechanical resonator. *Nat Nano*, 8(7):493–496, 2013.
- [11] Ya. M. Blanter, O. Usmani, and Yu. V. Nazarov. Single-Electron Tunneling with Strong Mechanical Feedback. *Phys. Rev. Lett.*, 93(13):136802, September 2004.
- [12] Ya. M. Blanter, O. Usmani, and Yu. V. Nazarov. Erratum: Single-Electron Tunneling with Strong Mechanical Feedback [Phys. Rev. Lett. 93, 136802 (2004)]. *Phys. Rev. Lett.*, 94(4):049904, 2005.
- [13] A. D. Armour, M. P. Blencowe, and Y. Zhang. Classical dynamics of a nanomechanical resonator coupled to a single-electron transistor. *Phys. Rev. B*, 69(12):125313, March 2004.
- [14] C. B. Doiron, W. Belzig, and C. Bruder. Electrical transport through a single-electron transistor strongly coupled to an oscillator. *Phys. Rev. B*, 74:205336, 2006.
- [15] F. Pistolesi and R. Shekhter. Tunable spin-polaron state in a singly clamped semiconducting carbon nanotube. *Phys. Rev. B*, 92(3):035423, 2015.
- [16] D. Mozyrsky, M. B. Hastings, and I. Martin. Intermittent polaron dynamics: Born-Oppenheimer approximation out of equilibrium. *Phys. Rev. B*, 73(3):035104, January 2006.
- [17] Jens Koch and Felix von Oppen. Franck-Condon Blockade and Giant Fano Factors in Transport through Single Molecules. *Phys. Rev. Lett.*, 94(20):206804, 2005.
- [18] F. Pistolesi and S. Labarthe. Current blockade in classical single-electron nanomechanical resonator. *Phys. Rev. B*, 76(16):165317, October 2007.
- [19] F. Pistolesi, Ya. M. Blanter, and Ivar Martin. Self-consistent theory of molecular switching. *Phys. Rev. B*, 78(8):085127, 2008.

-
- [20] F. Pistolesi. Cooling a Vibrational Mode Coupled to a Molecular Single-Electron Transistor. *Journal of Low Temperature Physics*, 154(5-6):199–210, March 2009.
- [21] Stefano Zippilli, Giovanna Morigi, and Adrian Bachtold. Cooling Carbon Nanotubes to the Phononic Ground State with a Constant Electron Current. *Phys. Rev. Lett.*, 102(9):096804, March 2009.
- [22] P. Stadler, W. Belzig, and G. Rastelli. Ground-State Cooling of a Carbon Nanomechanical Resonator by Spin-Polarized Current. *Phys. Rev. Lett.*, 113(4):047201, 2014.
- [23] N. M. Chtchelkatchev, W. Belzig, and C. Bruder. Charge transport through a single-electron transistor with a mechanically oscillating island. *Phys. Rev. B*, 70(19):193305, November 2004.
- [24] I. Mahboob, K. Nishiguchi, A. Fujiwara, and H. Yamaguchi. Phonon Lasing in an Electromechanical Resonator. *Phys. Rev. Lett.*, 110(12):127202, March 2013.
- [25] I. Mahboob, H. Okamoto, K. Onomitsu, and H. Yamaguchi. Two-Mode Thermal-Noise Squeezing in an Electromechanical Resonator. *Phys. Rev. Lett.*, 113(16):167203, October 2014.
- [26] G. Micchi, R. Avriller, and F. Pistolesi. Mechanical Signatures of the Current Blockade Instability in Suspended Carbon Nanotubes. *Phys. Rev. Lett.*, 115(20):206802, November 2015.
- [27] G. Micchi, R. Avriller, and F. Pistolesi. Electromechanical transition in quantum dots. *Phys. Rev. B*, 94(12):125417, September 2016.
- [28] Miles P. Blencowe and Martin N. Wybourne. Sensitivity of a micromechanical displacement detector based on the radio-frequency single-electron transistor. *Applied Physics Letters*, 77(23):3845, 2000.
- [29] A. Naik, O. Buu, M. D. LaHaye, A. D. Armour, A. A. Clerk, M. P. Blencowe, and K. C. Schwab. Cooling a nanomechanical resonator with quantum back-action. *Nature*, 443(7108):193–196, September 2006.
- [30] Robert G. Knobel and Andrew N. Cleland. Nanometre-scale displacement sensing using a single electron transistor. *Nature*, 424(6946):291–293, 2003.

- [31] Vera Sazonova, Yuval Yaish, Hande Üstünel, David Roundy, Tomás A. Arias, and Paul L. McEuen. A tunable carbon nanotube electromechanical oscillator. *Nature*, 431(7006):284–287, 2004.
- [32] B. Lassagne, Y. Tarakanov, J. Kinaret, D. Garcia-Sanchez, and A. Bachtold. Coupling Mechanics to Charge Transport in Carbon Nanotube Mechanical Resonators. *Science*, 325(5944):1107–1110, August 2009.
- [33] G. A. Steele, A. K. Hüttel, B. Witkamp, M. Poot, H. B. Meerwaldt, L. P. Kouwenhoven, and H. S. J. van der Zant. Strong Coupling Between Single-Electron Tunneling and Nanomechanical Motion. *Science*, 325(5944):1103–1107, August 2009.
- [34] H. B. Meerwaldt, G. Labadze, B. H. Schneider, A. Taspinar, Ya. M. Blanter, H. S. J. van der Zant, and G. A. Steele. Probing the charge of a quantum dot with a nanomechanical resonator. *Phys. Rev. B*, 86(11):115454, September 2012.
- [35] Marc Ganzhorn and Wolfgang Wernsdorfer. Dynamics and Dissipation Induced by Single-Electron Tunneling in Carbon Nanotube Nanoelectromechanical Systems. *Phys. Rev. Lett.*, 108(17):175502, 2012.
- [36] Marc Ganzhorn, Svetlana Klyatskaya, Mario Ruben, and Wolfgang Wernsdorfer. Carbon Nanotube Nanoelectromechanical Systems as Magnetometers for Single-Molecule Magnets. *ACS Nano*, 7(7):6225–6236, 2013.
- [37] Ben H. Schneider, Vibhor Singh, Warner J. Venstra, Harold B. Meerwaldt, and Gary A. Steele. Observation of decoherence in a carbon nanotube mechanical resonator. *Nature Communications*, 5:5819, December 2014.
- [38] Vincent Gouttenoire, Thomas Barois, Sorin Perisanu, Jean-Louis Leclercq, Stephen T. Purcell, Pascal Vincent, and Anthony Ayari. Digital and FM Demodulation of a Doubly Clamped Single-Walled Carbon-Nanotube Oscillator: Towards a Nanotube Cell Phone. *Small*, 6(9):1060–1065, 2010.
- [39] Ingold, G.-L. and Nazarov, Yu V. Charge Tunneling Rates in Ultrasmall Junctions. In *Single electron tunnelling*, volume 294 of *NATO ASI Series*, pages 21–107. Springer US, grabert, hermann and devoret, michel h. edition, 1992.

-
- [40] A. N. Korotkov. Intrinsic noise of the single-electron transistor. *Phys. Rev. B*, 49(15):10381–10392, 1994.
- [41] A. D. Armour. Current noise of a single-electron transistor coupled to a nanomechanical resonator. *Phys. Rev. B*, 70:165315, 2004.
- [42] O. Usmani, Ya M. Blanter, and Y. V. Nazarov. Strong feedback and current noise in nanoelectromechanical systems. *Phys. Rev. B*, 75:195312, 2007.
- [43] Guillaume Weick, Felix von Oppen, and Fabio Pistolesi. Euler buckling instability and enhanced current blockade in suspended single-electron transistors. *Phys. Rev. B*, 83(3):035420, January 2011.
- [44] A. A. Clerk. Quantum-limited position detection and amplification: A linear response perspective. *Phys. Rev. B*, 70(24):245306, 2004.
- [45] Jochen Brüggemann, Guillaume Weick, Fabio Pistolesi, and Felix von Oppen. Large current noise in nanoelectromechanical systems close to continuous mechanical instabilities. *Phys. Rev. B*, 85(12):125441, March 2012.
- [46] A. A. Clerk, M. H. Devoret, S. M. Girvin, Florian Marquardt, and R. J. Schoelkopf. Introduction to quantum noise, measurement, and amplification. *Rev. Mod. Phys.*, 82(2):1155–1208, 2010.
- [47] C. Bruder and H. Schoeller. Charging effects in ultrasmall quantum dots in the presence of time-varying fields. *Phys. Rev. Lett.*, 72(7):1076–1079, 1994.
- [48] A. Benyamini, A. Hamo, S. Viola Kusminskiy, F. von Oppen, and S. Ilani. Real-space tailoring of the electron–phonon coupling in ultraclean nanotube mechanical resonators. *Nature Physics*, 10(2):151–156, January 2014.
- [49] C. W. J. Beenakker. Theory of Coulomb-blockade oscillations in the conductance of a quantum dot. *Phys. Rev. B*, 44(4):1646–1656, 1991.
- [50] A. Hamo, A. Benyamini, I. Shapir, I. Khivrich, J. Waissman, K. Kaasbjerg, Y. Oreg, F. von Oppen, and S. Ilani. Electron attraction mediated by Coulomb repulsion. *Nature*, 535(7612):395–400, 2016.

-
- [51] Ya. M. Blanter and M. Büttiker. Shot noise in mesoscopic conductors. *Physics Reports*, 336(1–2):1–166, September 2000.
- [52] Yue Wang and Fabio Pistoiesi. Sensitivity of mixing-current technique to detect nanomechanical motion. *Phys. Rev. B*, 95(3):035410, January 2017.
- [53] S. Stapfner, L. Ost, D. Hunger, J. Reichel, I. Favero, and E. M. Weig. Cavity-enhanced optical detection of carbon nanotube Brownian motion. *Applied Physics Letters*, 102(15):151910, April 2013.